

## Supporting Information

### Fabrication of MMMs with improved gas separation properties using externally-functionalized MOF particles

*Surendar R Venna<sup>1,2</sup>, Michael Lartey<sup>1,6</sup>, Tao Li<sup>3</sup>, Alex Spore<sup>3</sup>, Santosh Kumar<sup>1,6</sup>, Hunaid B Nulwala<sup>1,4</sup>, David R Luebke<sup>1</sup>, Nathaniel L Rosi<sup>3,\*</sup>, Erik Albenze<sup>1,5,\*</sup>*

<sup>1</sup>National Energy Technology Laboratory, Pittsburgh, PA 15236; <sup>2</sup>West Virginia University Research Corporation, Morgantown, WV 26506; <sup>3</sup>University of Pittsburgh, Pittsburgh, PA 15260; <sup>4</sup>Carnegie Mellon University, Pittsburgh, PA 15213; <sup>5</sup>URS Energy and Construction, Pittsburgh, PA 15236; <sup>6</sup>Oak Ridge Institute for Science and Education, Oak Ridge, TN 37831

E-mail: erik.albenze@netl.doe.gov, nrosi@pitt.edu

#### Table of Contents:

1. Safety Note
2. Compound Characterization (Figures S1-S9, Tables S1-S4)
3. Low-Pressure Gas Adsorption Measurements (Figure S10-S14)
4. Preparation of MOFs for Membrane Studies (Figures S15-S19)
5. MMM Characterization and Performance (Figures S20-S26)
6. Raw Sorption Data Tables

## **1. Safety Note**

HF is highly corrosive and dangerous in both liquid and gas phases. HF can cause burns that are dangerous and may or may not be immediately visible or painful. Furthermore, if swallowed or inhaled, HF can be fatal. The liquid and vapor can burn and/or severely harm eyes, skin, or respiratory tract. HF is known to cause bone damage. Consult your MSDS for further details. USE CAUTIOUSLY.

## 2. Compound Characterization

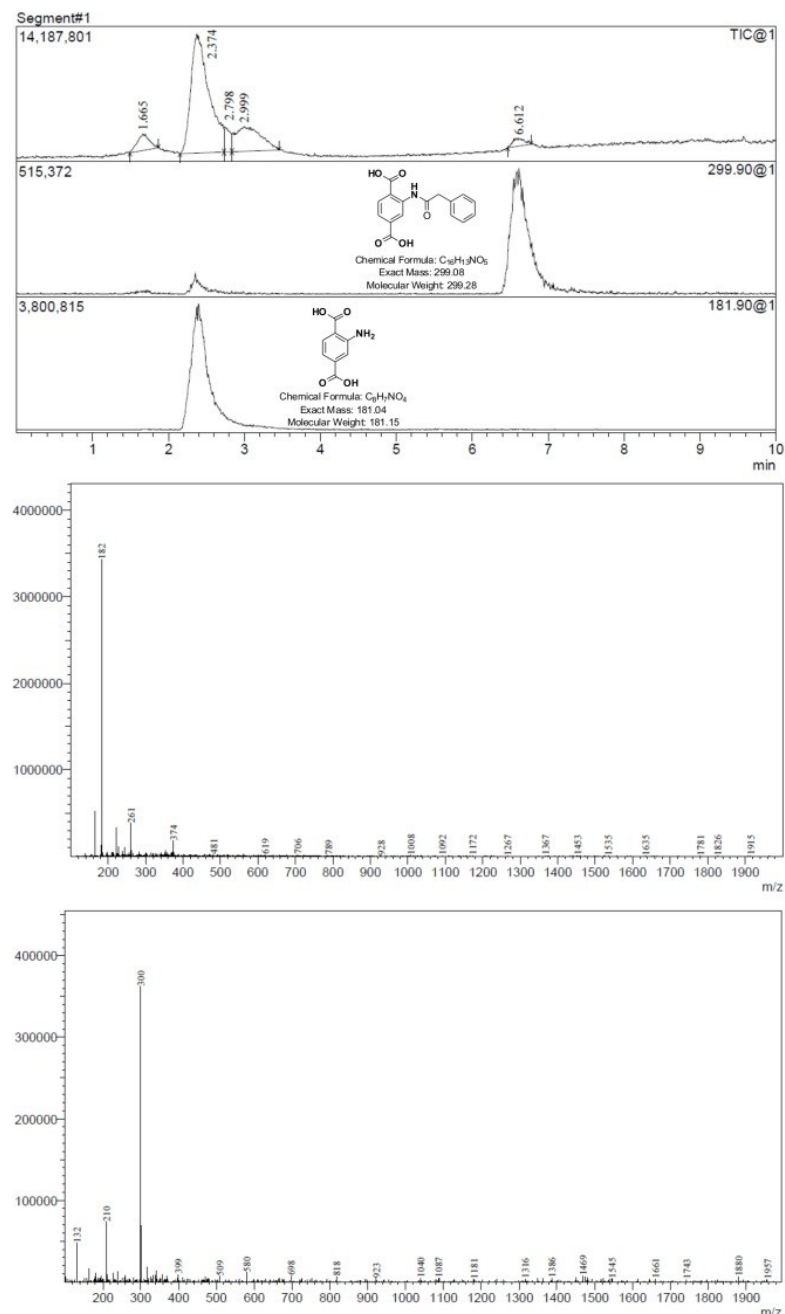


**Figure S1:** LCMS data of digested **I<sub>PA</sub>**. The unfunctionalized ligand (mw = 181 g/mol) elutes at 2.3 min (MS middle) while the phenyl acetyl functionalized ligand (mw = 299 g/mol) elutes at 6.6 min (MS bottom).

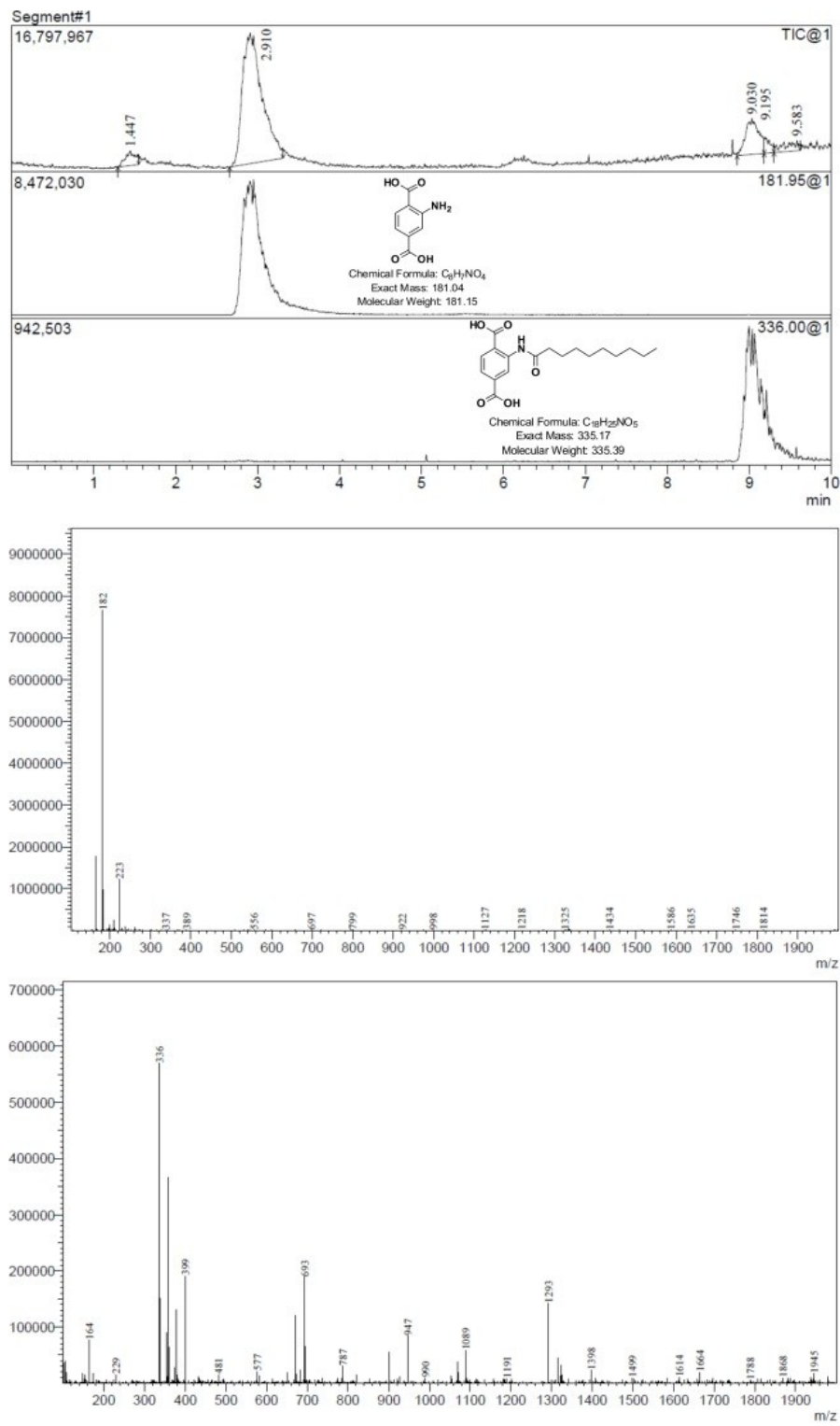


**Figure S2:** LCMS data of digested **I<sub>C10</sub>**. The unfunctionalized ligand (mw = 181 g/mol) elutes at 2.9 min (MS middle) while the decanoyl acetyl functionalized ligand (mw = 335 g/mol) elutes at 9.0 min (MS bottom).

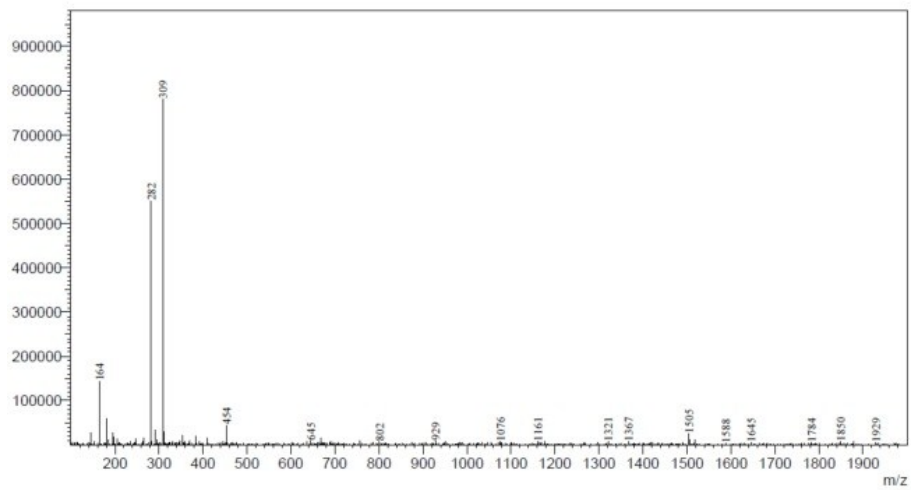
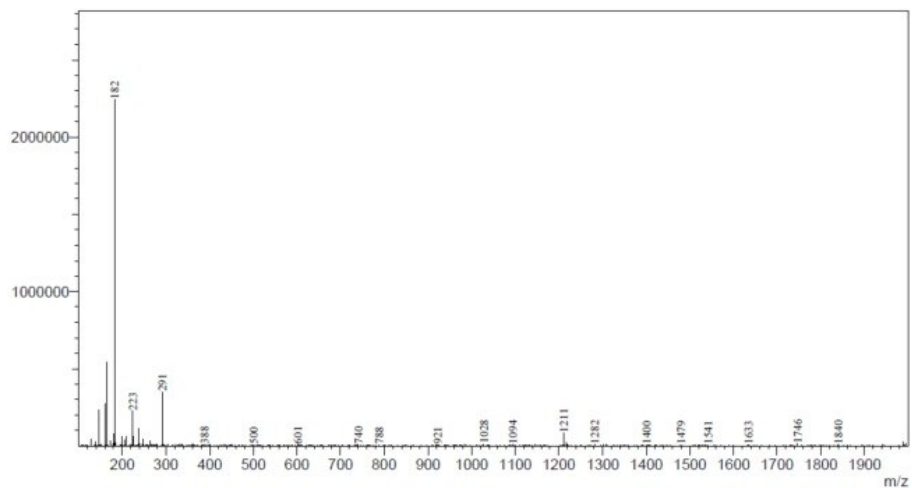
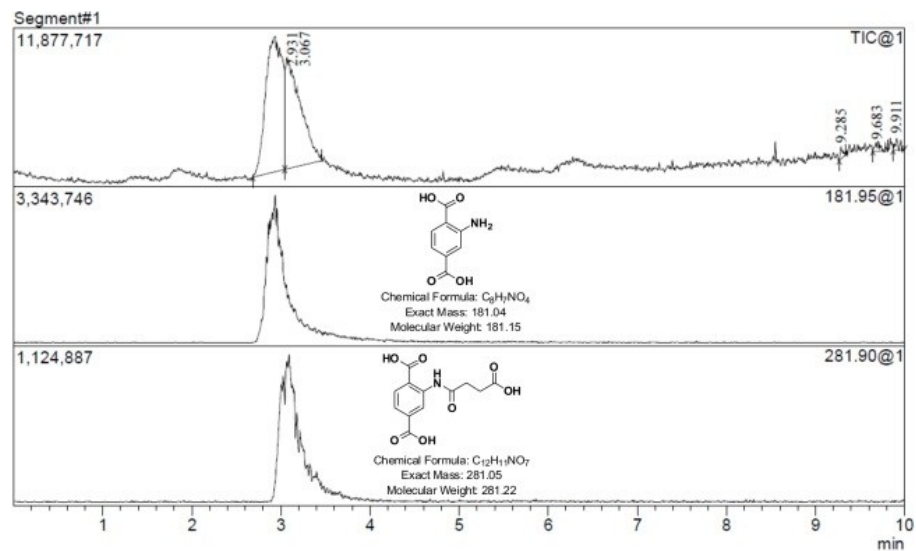


**Figure S3:** LCMS data of digested **I<sub>SA</sub>**. The unfunctionalized ligand (mw = 181 g/mol) elutes at 2.9 min (MS middle) while the succinic acid functionalized ligand (mw = 281 g/mol) elutes at 3.0 min (MS bottom).

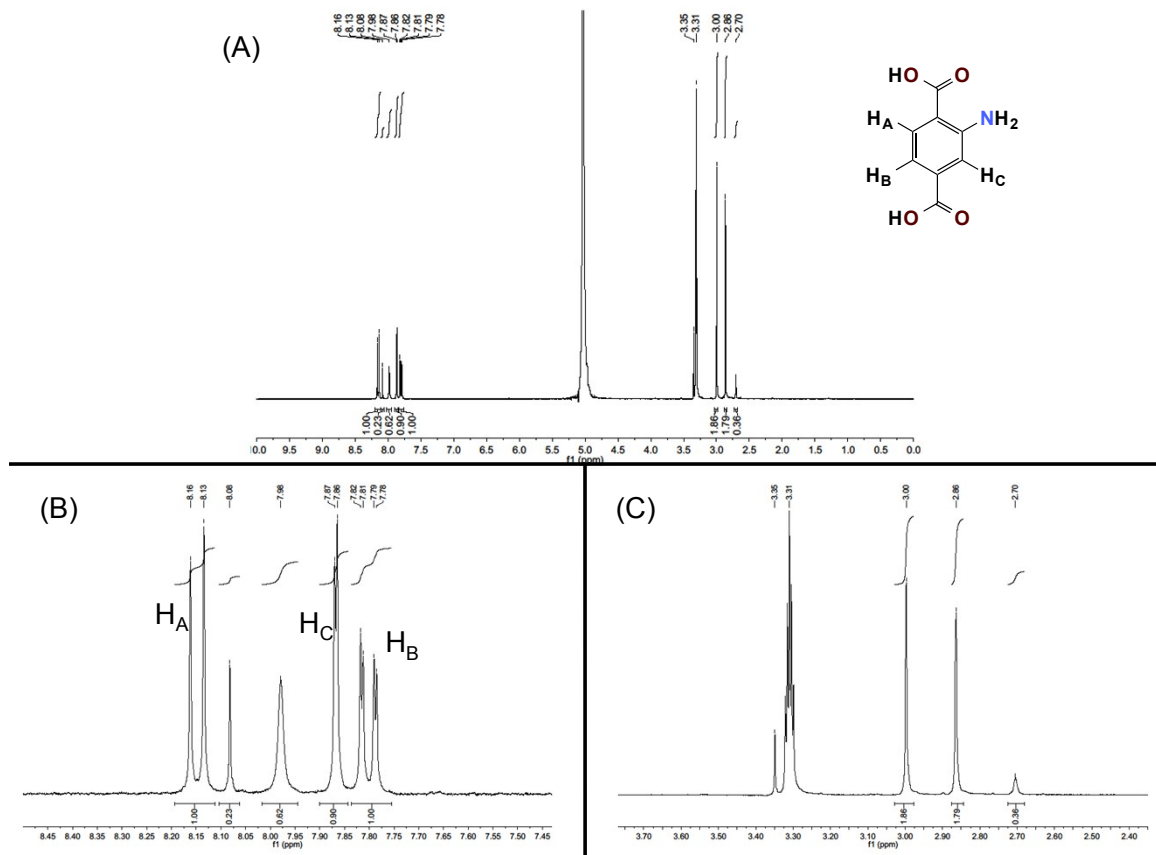


**Figure S4:**  $^1\text{H}$  NMR spectrum of digested **I** (A) and a magnified region (B & C). See **Table S1** for signal shifts, integrations, and assignments.

**Table S1.**  $^1\text{H}$  NMR signal shifts, integration and assignments for **I**.

Proton	Chemical Shift, ppm (splitting)	Predicted Integration	Actual Integration
H <sub>A</sub>	8.14 (doublet)	1 H	1.00 H
H <sub>B</sub>	7.80 (doublet)	1 H	1.00 H
H <sub>C</sub>	7.86 (singlet)	1 H	0.90 H
DMF	7.98 (singlet)	--	0.62 H
DMF	2.86 and 3.00 (singlets)	--	1.83 H
CHCl <sub>3</sub>	8.08 (singlet)	--	0.23 H
H <sub>2</sub> O & HF	5.00 (singlet)	--	--
MeOH	3.31 (singlet)	--	--

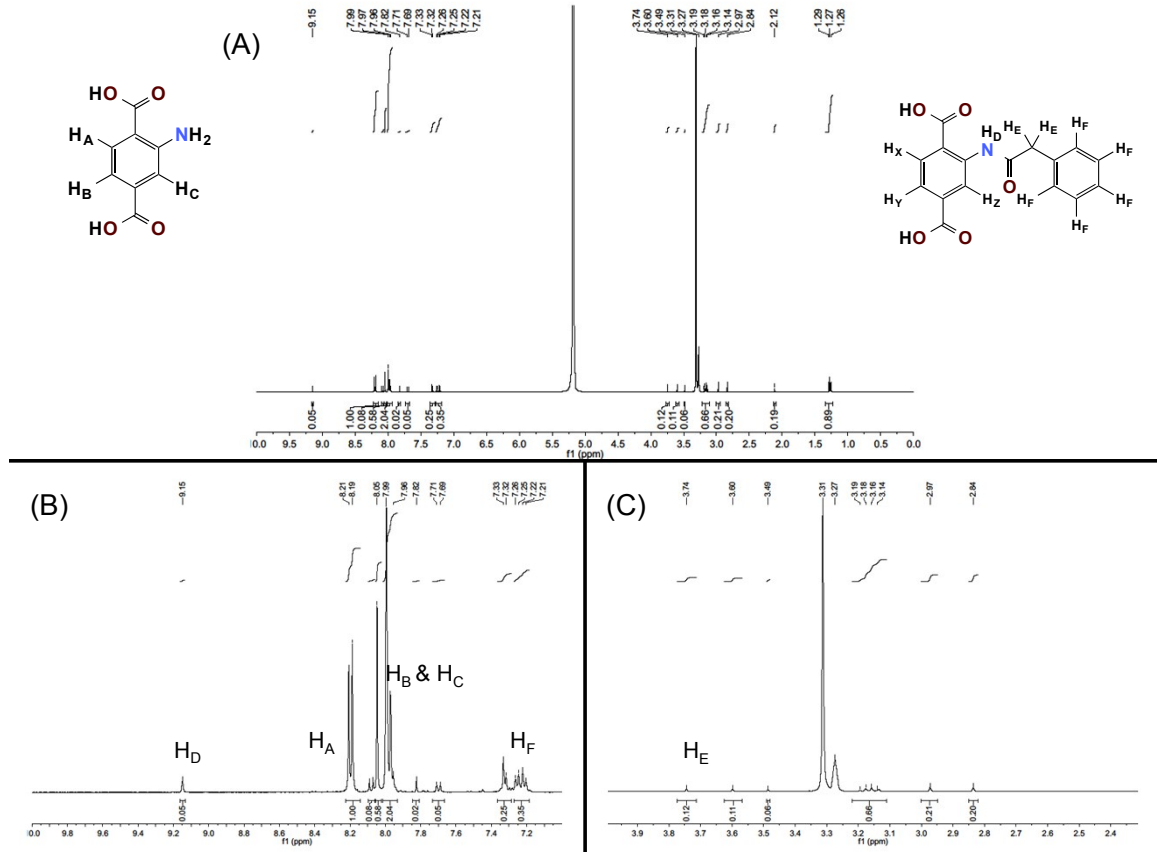


**Figure S5:**  $^1\text{H}$  NMR spectrum of digested **I<sub>PA</sub>**. Degree of functionalization determined by calculating the integration ratio between H<sub>2</sub>-NH<sub>2</sub>-BDC (H<sub>A</sub>) to amide proton (H<sub>D</sub>). **I<sub>PA</sub>** was functionalized 5% in this sample and functionalization ranged from 3-6%. Some free phenylacetyl chloride is observed (H<sub>E</sub> and H<sub>F</sub>). See **Table S4** for signal shifts, integrations, and assignments.

**Table S2:**  $^1\text{H}$  NMR signal shifts, integration and assignments for  $\mathbf{I}_{\text{PA}}$ .

Proton	Chemical Shift, ppm (splitting)	Predicted Integration	Actual Integration	Percent Functionalization
H <sub>A</sub>	8.20 (doublet)	1 H	1.00 H	--
H <sub>B</sub> & H <sub>C</sub>	7.97 (multiplet)	2 H	2.04 H	--
H <sub>D</sub>	9.15 (singlet)	--	0.05 H	5%
H <sub>E</sub>	3.74 (singlet)	--	0.12 H	--
H <sub>E</sub> (Free)	3.60 (singlet)	--	0.11 H	--
H <sub>F</sub>	7.32 (multiplet)	--	0.25 H	--
H <sub>F</sub> (Free)	7.23 (multiplet)	--	0.35 H	--
H <sub>X</sub>	8.07 (doublet)	--	0.08 H	--
H <sub>Y</sub>	7.70 (doublet)	--	0.05 H	--
H <sub>Z</sub>	7.82 (singlet)	--	0.02 H	--
DMF	2.84 & 2.97 (singlets)	--	0.20 H	--
CHCl <sub>3</sub>	8.05 (singlet)	--	0.58 H	--
H <sub>2</sub> O & HF	5.00 (singlet)	--	--	--
MeOH	3.31 (singlet)	--	--	--

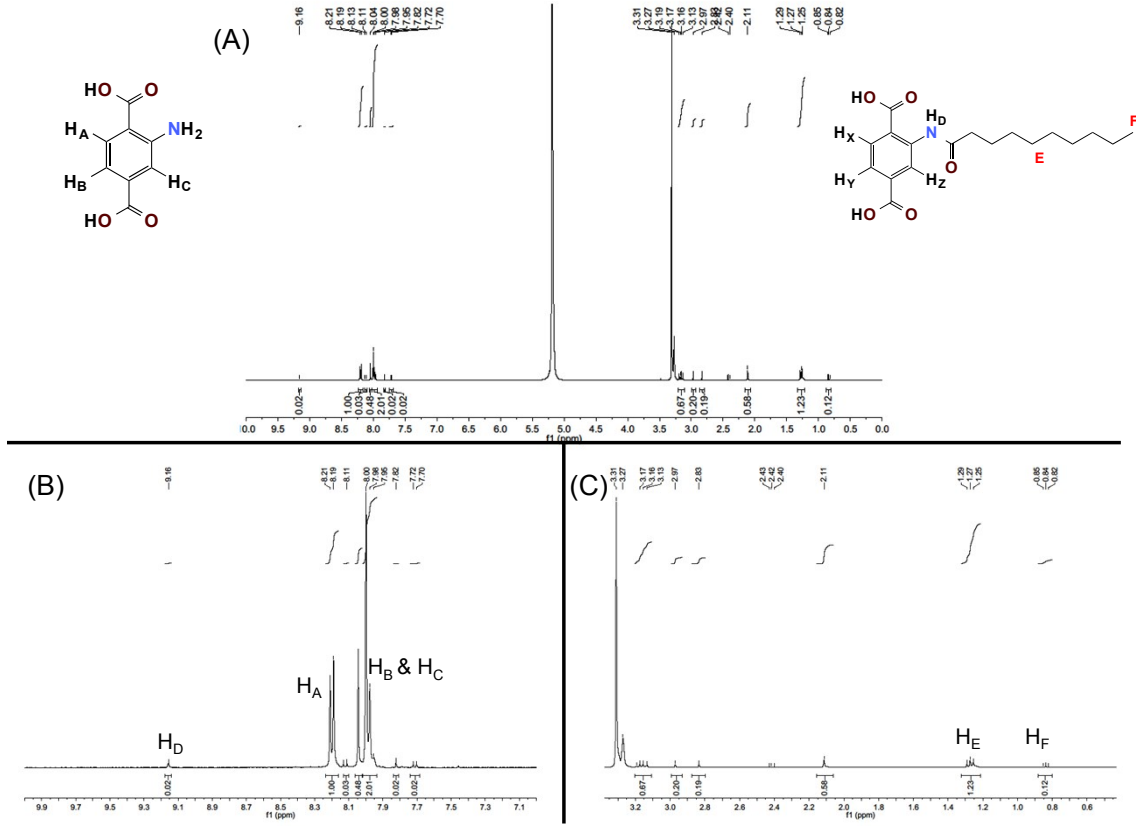


**Figure S6:**  $^1\text{H}$  NMR spectrum of digested  $\mathbf{I}_{\text{C}10}$ . Degree of functionalization determined by calculating the integration ratio between  $\text{H}_2\text{-NH}_2\text{-BDC}$  ( $\text{H}_\text{A}$ ) to amide proton ( $\text{H}_\text{D}$ ).  $\mathbf{I}_{\text{C}10}$  was functionalized 2% in this sample and ranged from 2-5%. We observe higher than expected integrations for  $\text{H}_\text{E}$  and  $\text{H}_\text{F}$ , which we attribute to the presence of free decanoyl chloride. See **Table S3** for signal shifts, integrations, and assignments.

**Table S3:**  $^1\text{H}$  NMR signal shifts, integration and assignments for **I<sub>C10</sub>**.

Proton	Chemical Shift, ppm (splitting)	Predicted Integration	Actual Integration	Percent Functionalization
H <sub>A</sub>	8.20 (doublet)	1 H	1.00 H	--
H <sub>B</sub> & H <sub>C</sub>	7.98 (multiplet)	2 H	2.01 H	--
H <sub>D</sub>	9.16 (singlet)	--	0.02 H	2%
H <sub>E</sub>	1.27 (multiplet)	--	1.23 H	--
H <sub>F</sub>	0.84 (triplet)	--	0.12 H	--
H <sub>X</sub>	8.11 (doublet)	--	0.03 H	--
H <sub>Y</sub>	7.71 (doublet)	--	0.02 H	--
H <sub>Z</sub>	7.82 (singlet) 2.83 & 2.97 (singlets)	--	0.02 H 0.19 H	--
CHCl <sub>3</sub>	8.05 (singlet)	--	0.48 H	--
H <sub>2</sub> O & HF	5.00 (singlet)	--	--	--
MeOH	3.31 (singlet)	--	--	--

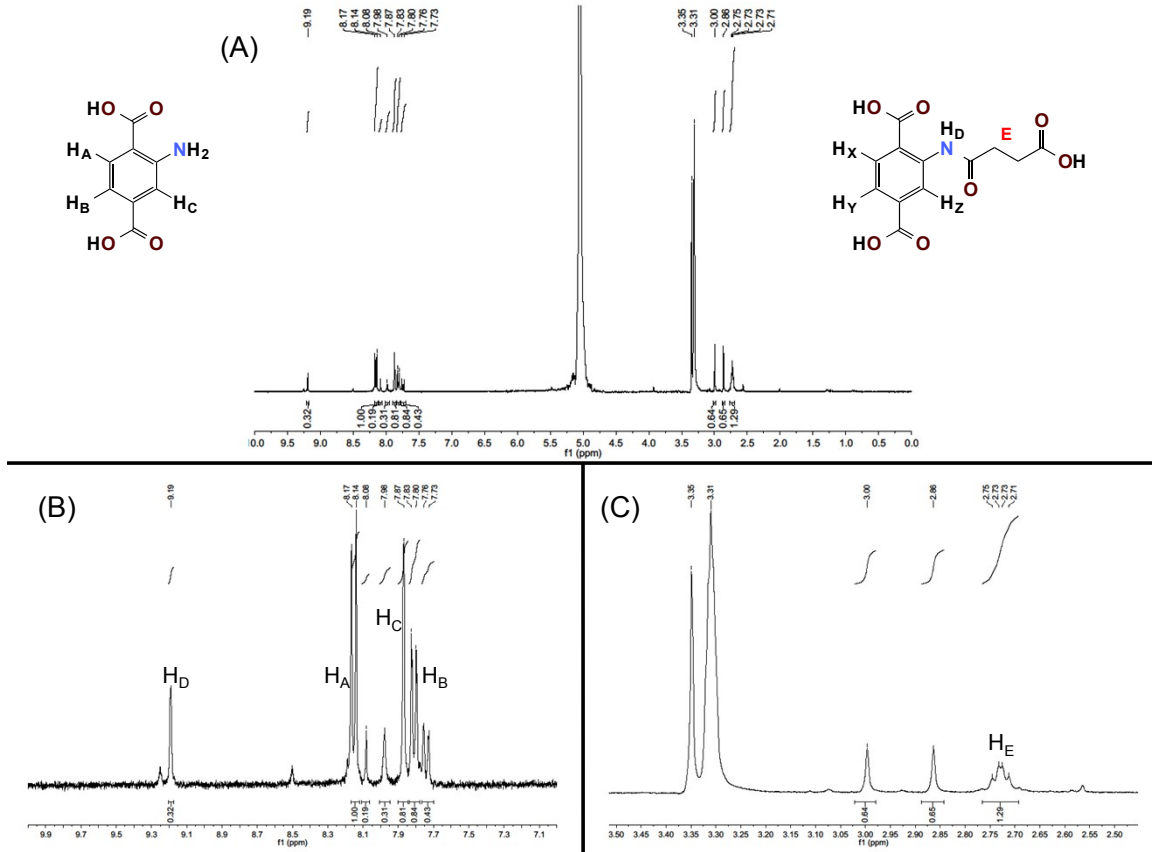


**Figure S7:**  $^1\text{H}$  NMR spectrum of digested  $\text{I}_{\text{SA}}$ . Degree of functionalization determined by calculating the integration ratio between  $\text{H}_2\text{-NH}_2\text{-BDC}$  ( $\text{H}_\text{A}$ ) to amide proton ( $\text{H}_\text{D}$ ).  $\text{I}_{\text{SA}}$  was functionalized 32% in this sample and ranged from 16-32%. See **Table S2** for signal shifts, integrations, and assignments.

**Table S4:**  $^1\text{H}$  NMR signal shifts, integration and assignments for  $\mathbf{I}_{\text{SA}}$ .

Proton	Chemical Shift, ppm (splitting)	Predicted Integration	Actual Integration	Percent Functionalization
H <sub>A</sub>	8.16 (doublet)	1 H	1.00 H	--
H <sub>B</sub>	7.78 (doublet)	1 H	0.84 H	--
H <sub>C</sub>	7.87 (singlet)	1 H	0.81 H	--
H <sub>D</sub>	9.19 (singlet)	--	0.32 H	32%
H <sub>E</sub>	2.73 (multiplet)	--	1.29 H	--
H <sub>Y</sub>	7.74 (doublet)	--	0.43 H	--
DMF	7.98 (singlet)	--	0.31 H	--
DMF	2.86 & 3.00 (singlets)	--	0.64 H	--
H <sub>2</sub> O & HF	5.00 (singlet)	--	--	--
MeOH	3.31 (singlet)	--	--	--

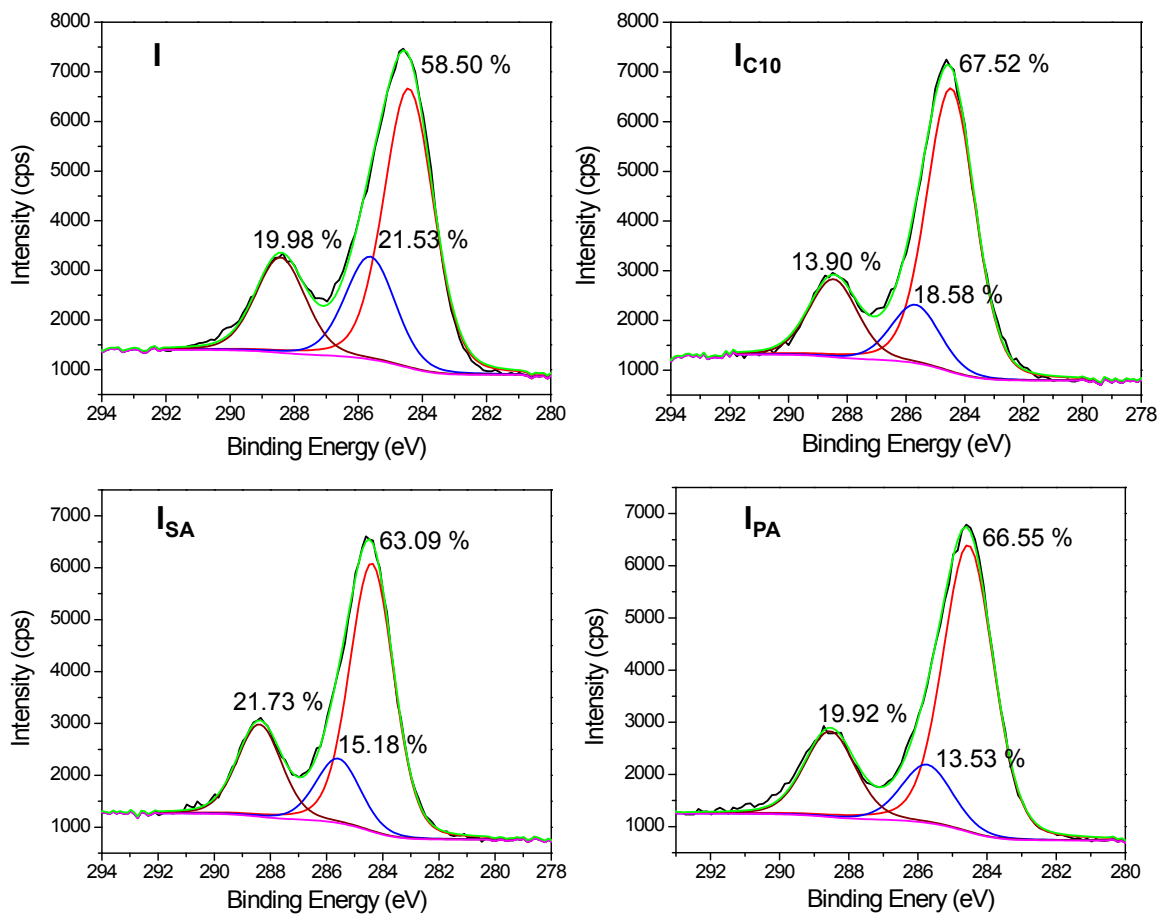


**Figure S8.** C 1s peak for functionalized MOFs before crushing. Black, actual curve; green, fitting to the curve; red, C-C/C=C peak; brown, COOH peak; blue, C-O/C-N peak; pink, background.

The analysis of C 1s data for the functionalized MOFs clearly verifies the surface functionalization. By fitting the C 1s data and analyzing the peak for C-C/C=C, C-O/C-N, and COOH, the percent of each bonding state of the carbon in the functionalized MOFs was obtained as shown in Figure S8. **I<sub>C10</sub>**, which has the most C-C bonds, showed the highest percent of C-C bond (67.52 %) followed by **I<sub>PA</sub>** (66.55 %), which has next highest number of C-C and C=C groups due to the presence of phenyl substituent. The COOH bonding state also provides proof of surface functionalization: **I<sub>SA</sub>** showed the highest % of COOH bonding state (21.73 %).

Crushing the surface-functionalized MOFs should expose their inner cores, which contain NH<sub>2</sub>-BDC. Therefore, the percent composition of each bonding state in all of the crushed MOFs should be very similar as shown in Figure S9. It is important to note that a slight difference in the bonding state for some of the MOFs could be due to incomplete crushing, or the X-ray hitting the surface functionalized groups.

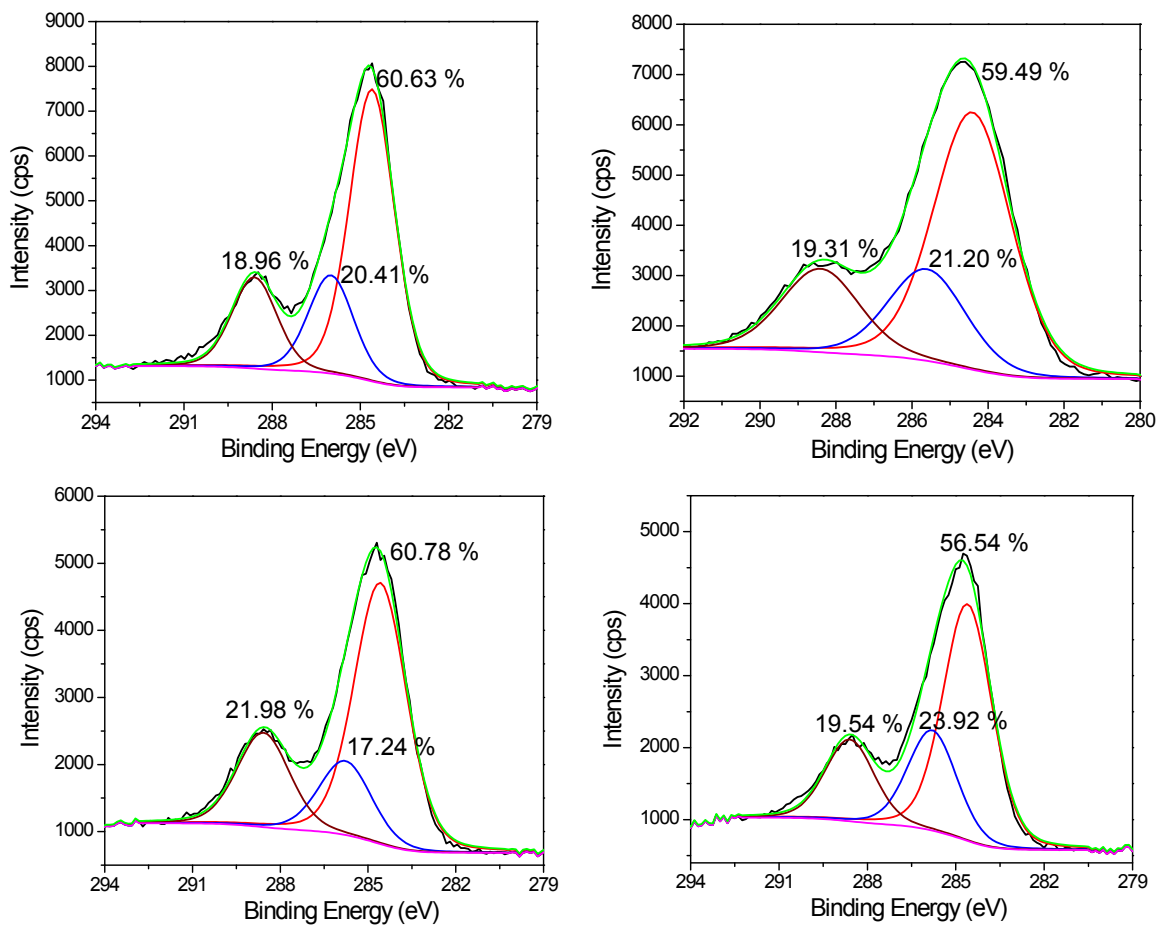


**Figure S9.** C 1s peak for functionalized MOFs after crushing. Black, actual curve; green, fitting to the curve; red, C-C/C=C peak; brown, COOH peak; blue, C-O/C-N peak; pink, background.

### 3. Low-Pressure Gas Adsorption Measurements

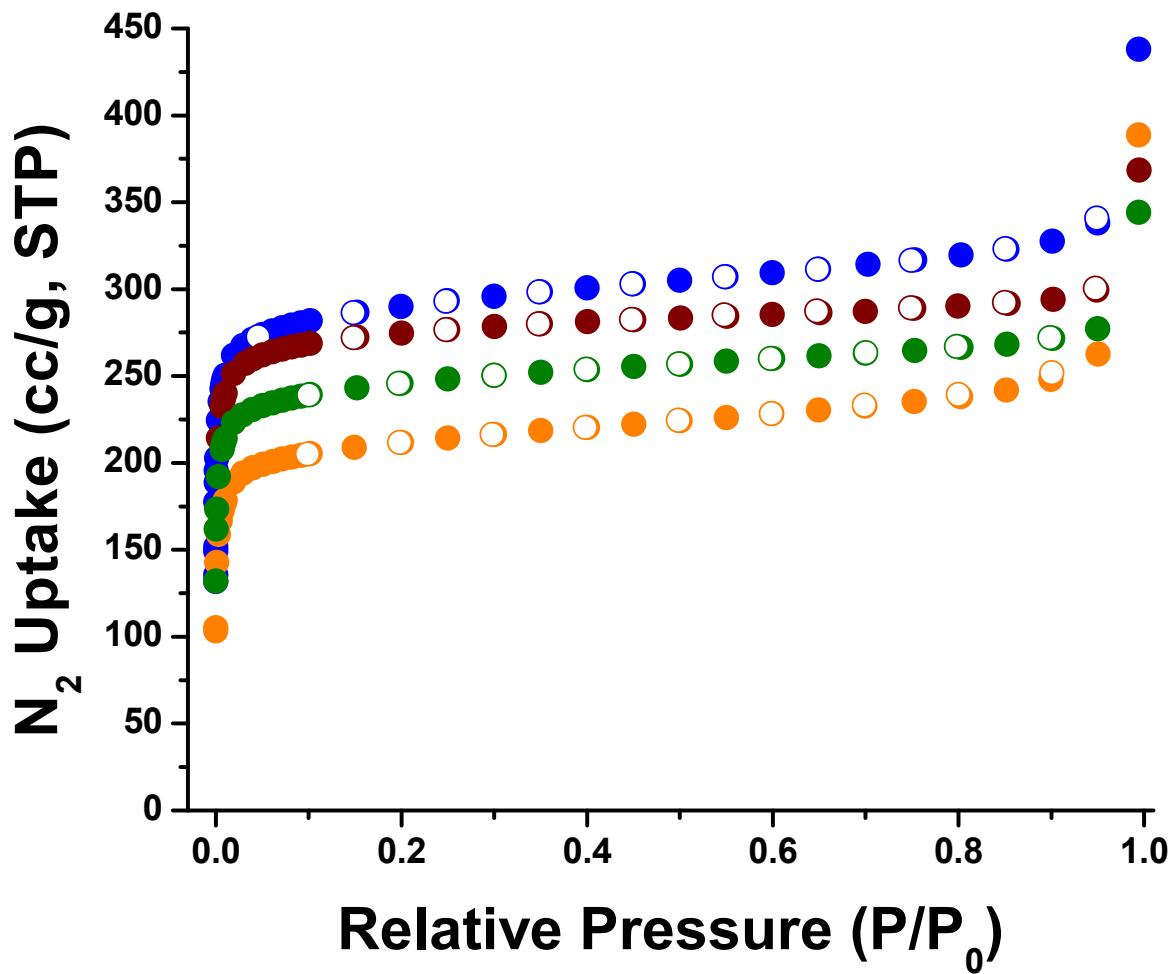


**Figure S10:** N<sub>2</sub> Isotherms (77 K) of **I** (blue), **IP<sub>A</sub>** (green), **IC<sub>10</sub>** (maroon), and **IS<sub>A</sub>** (orange). The N<sub>2</sub> uptake values at saturation reflect the degree of functionalization calculated for each of the modified materials.

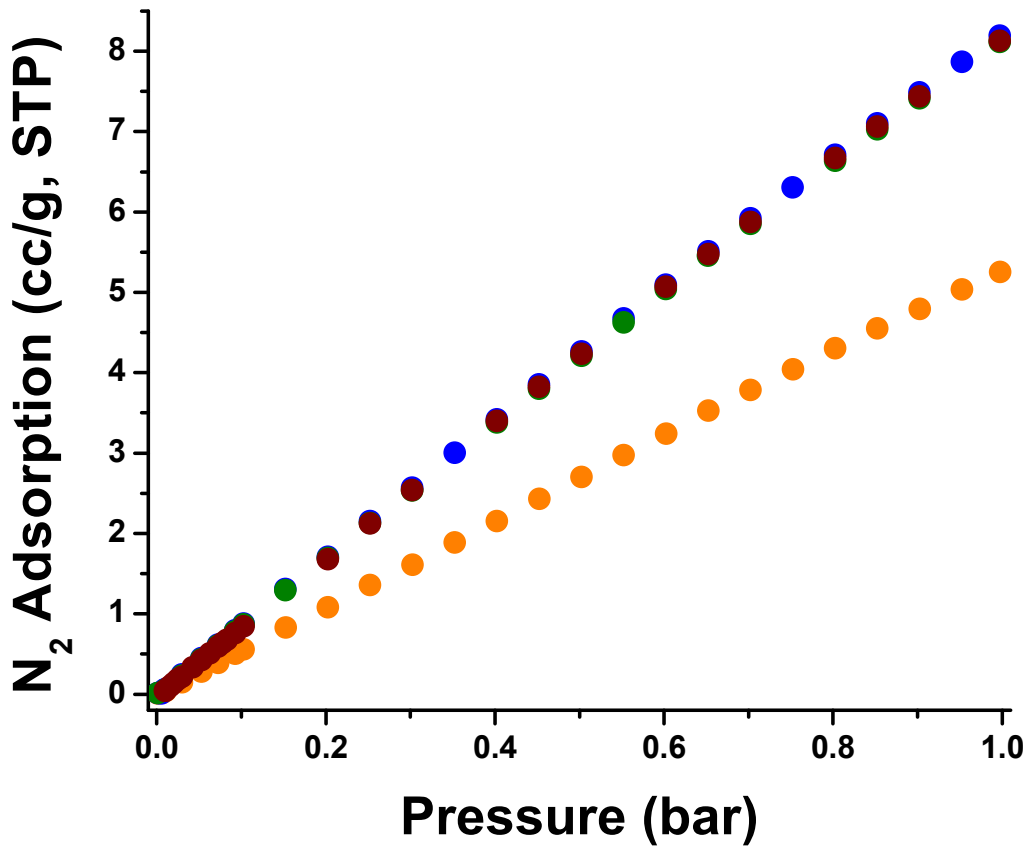


**Figure S11:** N<sub>2</sub> Isotherms (273 K) of **I** (blue), **IPA** (green), **IC<sub>10</sub>** (maroon), and **ISA** (orange).

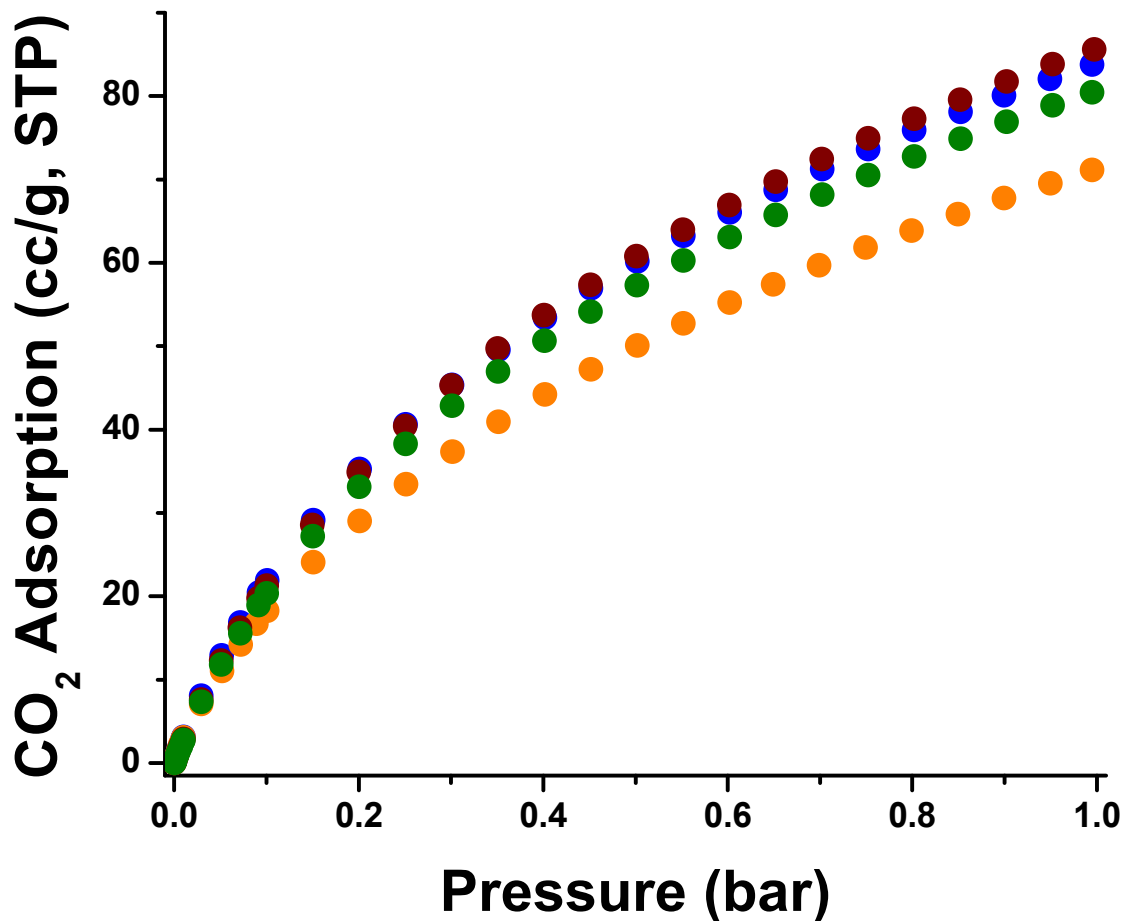


**Figure S12:** CO<sub>2</sub> isotherms (273 K) of I (blue), I<sub>PA</sub> (green), I<sub>C10</sub> (maroon), and I<sub>SA</sub> (orange).

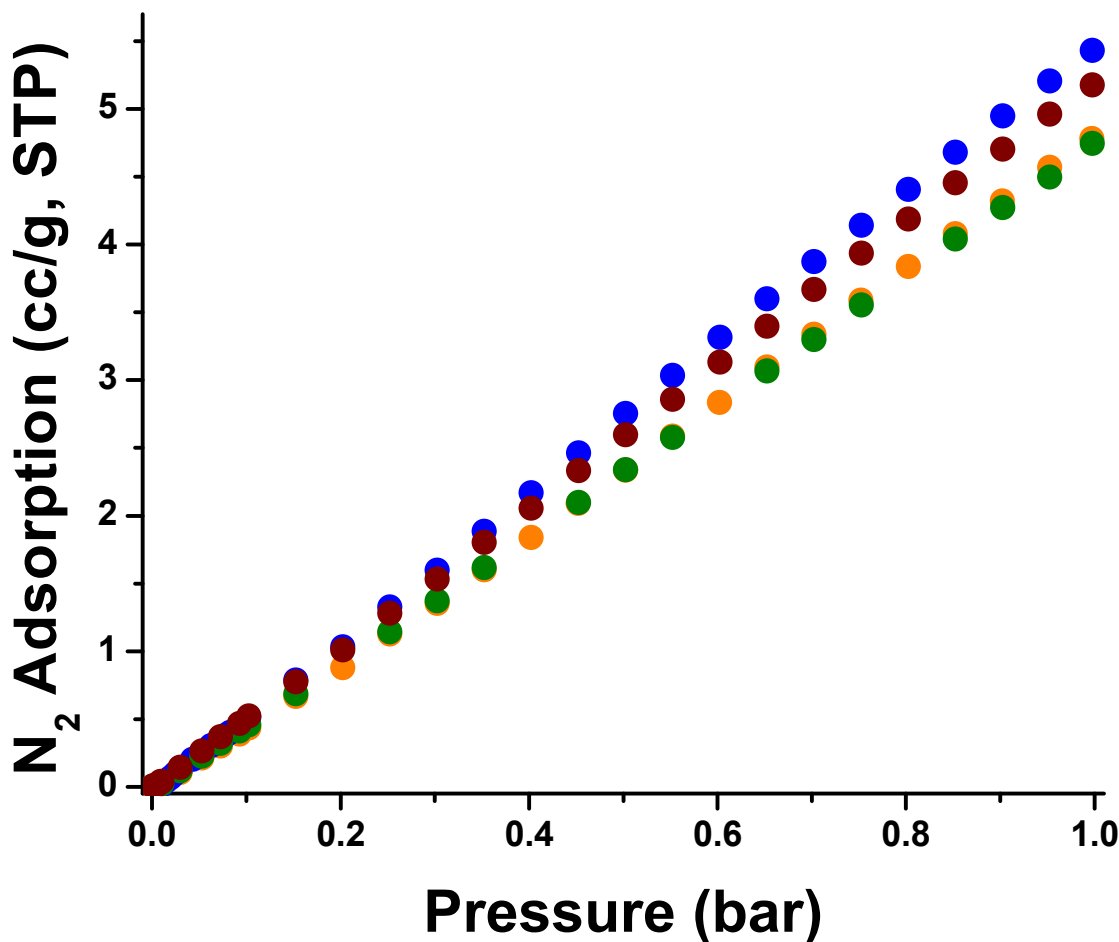


**Figure S13:** N<sub>2</sub> Isotherms (298 K) of I (blue), I<sub>PA</sub> (green), I<sub>C10</sub> (maroon), and I<sub>SA</sub> (orange).

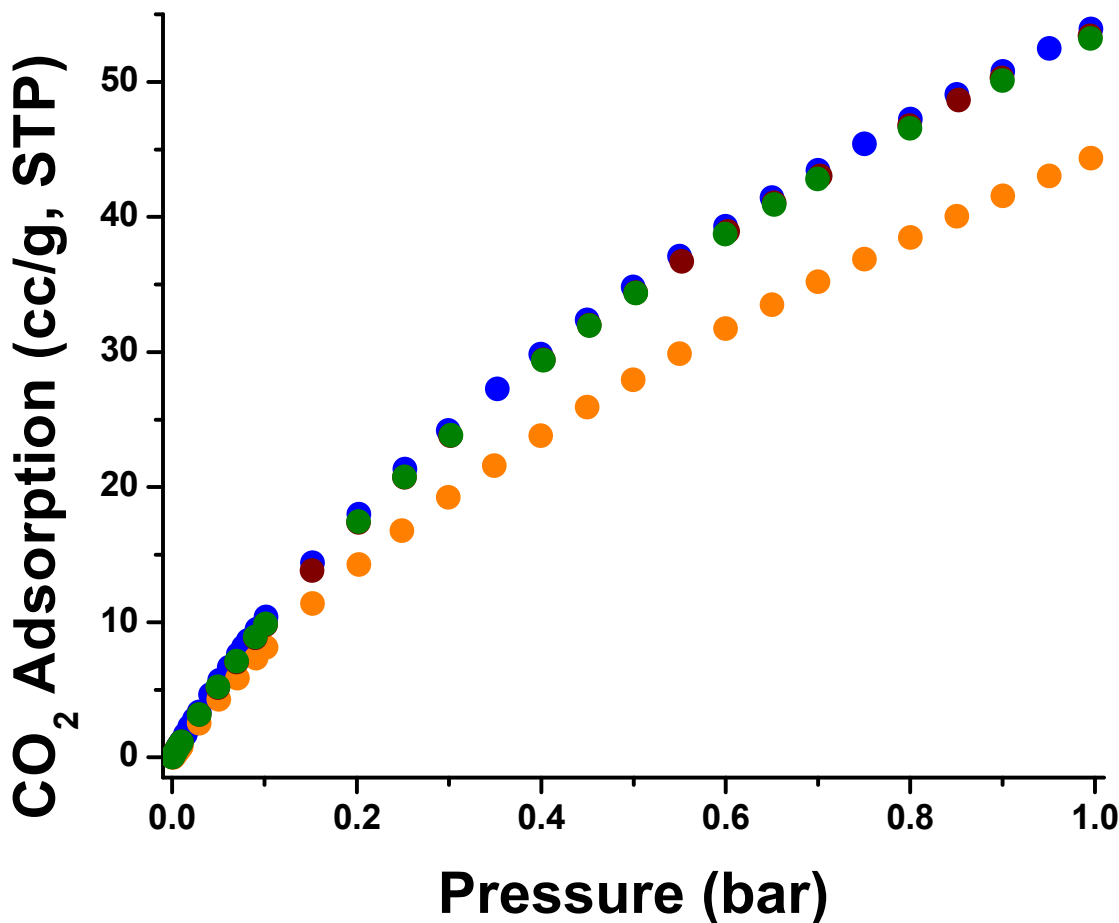


**Figure S14:** CO<sub>2</sub> isotherms (298 K) of I (blue), I<sub>PA</sub> (green), I<sub>C10</sub> (maroon), and I<sub>SA</sub> (orange).

## 4. Preparation of MOFs for Membrane Studies

**Compound Activation.** ~8-10g of MOF sample was placed in a single neck 250mL round-bottom flask. The flask was heated (200°C) under vacuum (20-30 mTorr) for 12 h. <sup>1</sup>H NMR spectra of dissolved activated MOF (see dissolution procedure in **Experimental Section**) were collected (Figure S15). These data reveal that only a very small amount of DMF (<1 molecule per Zr<sub>6</sub>O<sub>4</sub>(OH)<sub>4</sub>(NH<sub>2</sub>-BDC)<sub>6</sub> formula unit remains in the material after activation). The activated MOFs maintain their original crystallinity, as evidenced by PXRD (Figure S16). TGA studies were performed for **I** and activated **I** (Figure S17). The data reveal a significantly smaller weight loss step between 100-200°C for activated **I** compared to unactivated **I**, as expected. TGA studies were also performed for each of the activated functionalized samples (Figure S18).

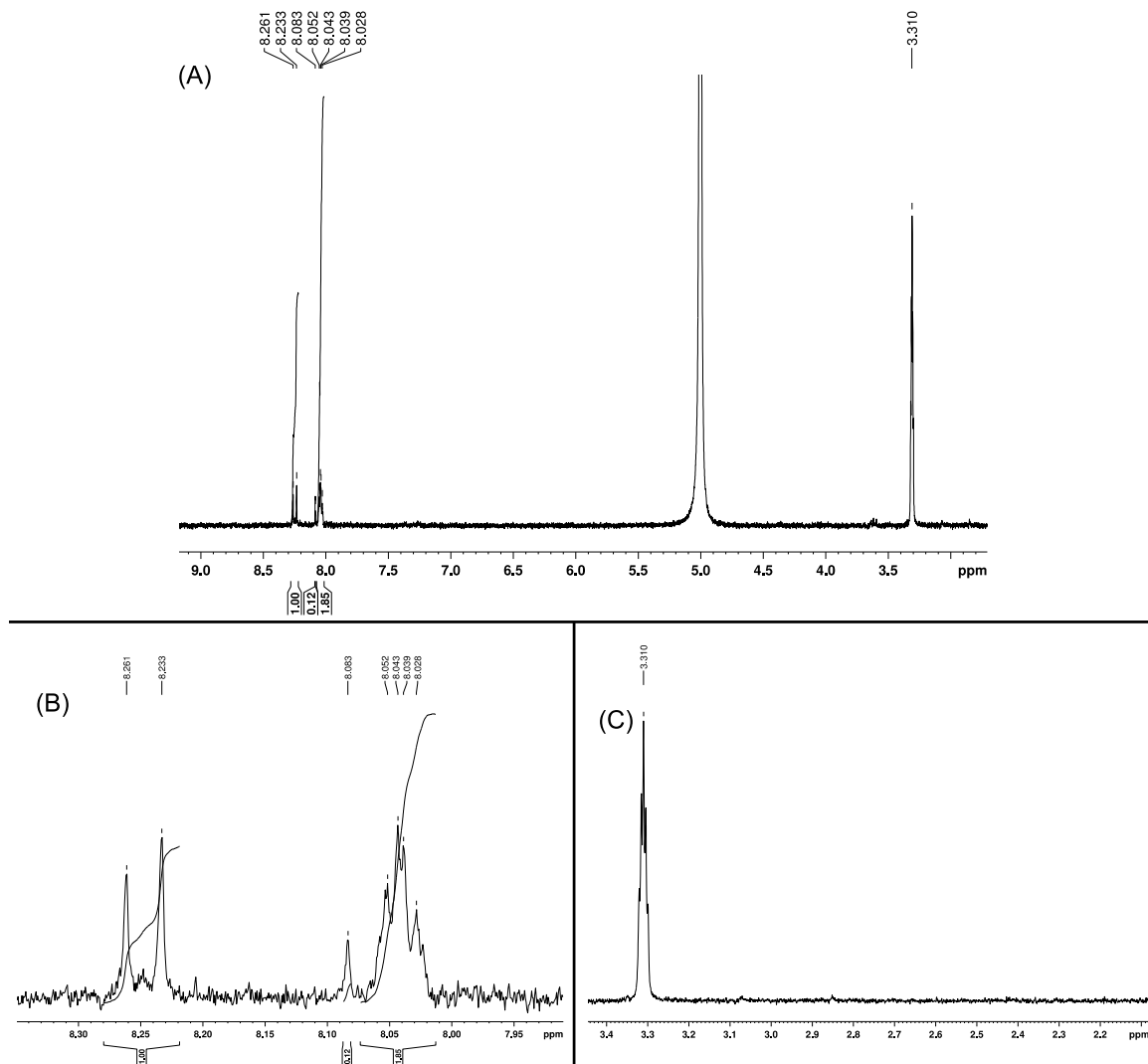


**Figure S15:** <sup>1</sup>H NMR of digested activated **I**. The signals for the DMF methyl protons (2.9 and 2.8 ppm), indicating that this activation procedure removes the DMF from the pores.

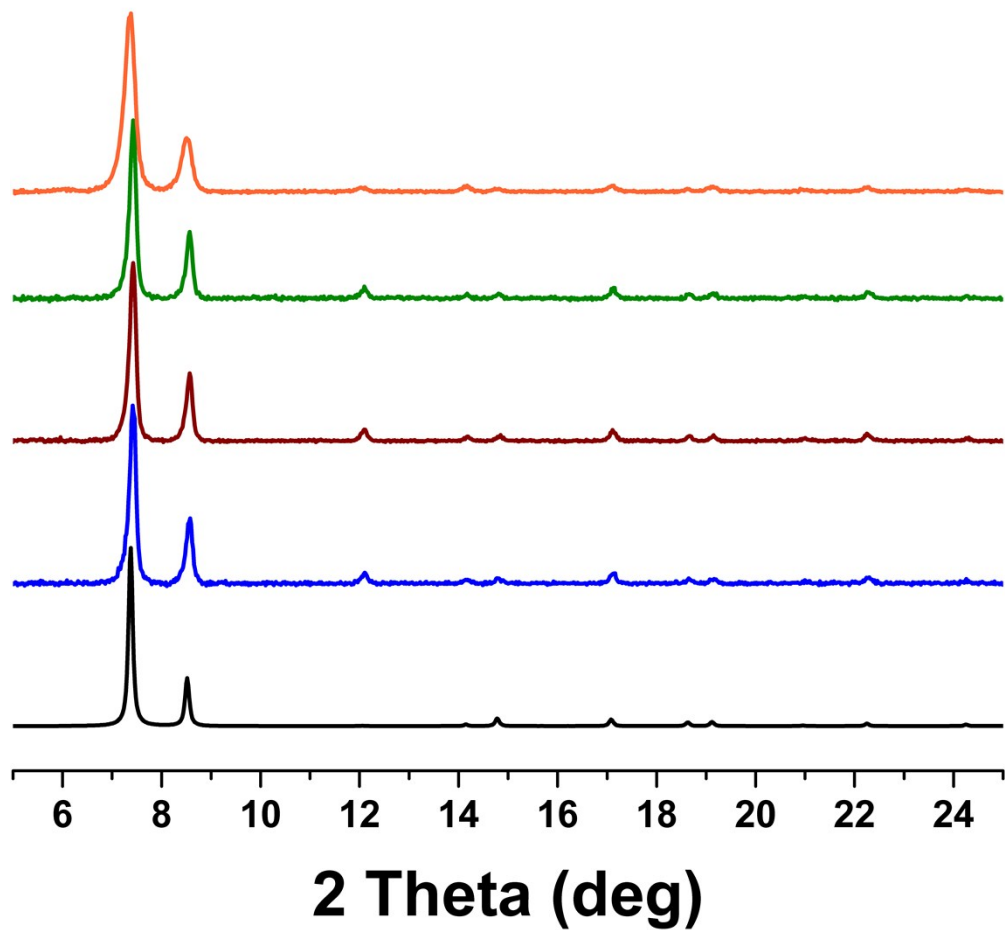


**Figure S16:** PXRD patterns for the simulated **I** (black), activated **I** (blue), activated **IC<sub>10</sub>** (maroon), activated **IPA** (green), and activated **ISA** (orange).

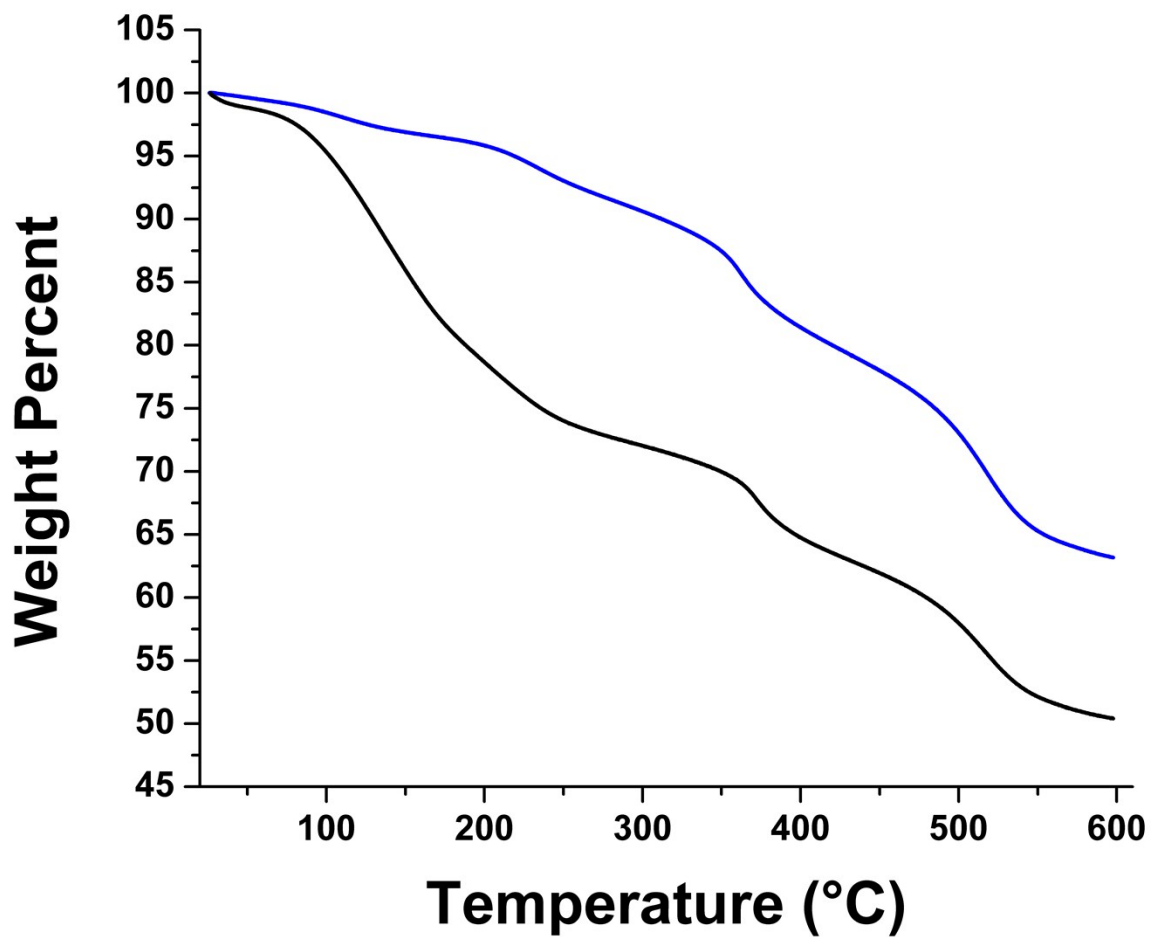


**Figure S17:** Thermal gravimetric analysis of activated I (blue) and I before activation (black).

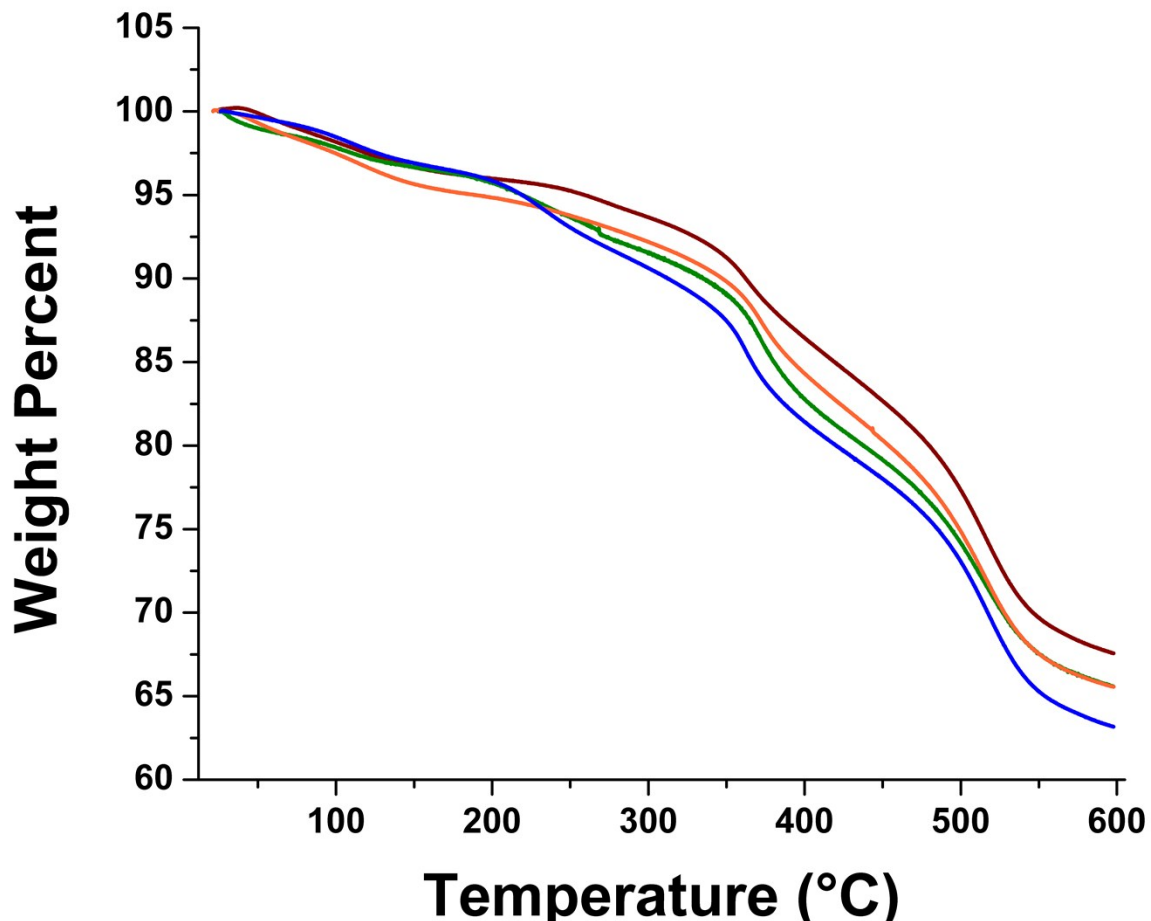


**Figure S18:** Thermal gravimetric analysis of activated **I** (blue), activated **IC<sub>10</sub>** (maroon), activated **IPA** (green), and activated **ISA** (orange).

We note that the activation procedure described above at the beginning of this section is different than the activation procedure used for the gas adsorption measurements reported in **Section 3** and described in the **Experimental Section**. To verify that the two activation procedures yield comparable activated product, we activated **I** on the Autosorb instrument at 200 °C under vacuum until the outgas rate was no more than 3 mTorr/min. We then measured the N<sub>2</sub> (77 K) adsorption isotherm of activated **I**. After collecting these isotherms, we compared them with the isotherm reported in **Section 3** (recall: **I** activated at 150 °C, Figures S10-S14). These N<sub>2</sub> isotherms collected at 77 K are overlaid in Figure S19. It is clear that the different activation procedures result in materials with comparable porosity and surface area (150 °C activation, BET SA=1135 m<sup>2</sup>/g; 200 °C activation, BET SA=1108 m<sup>2</sup>/g).

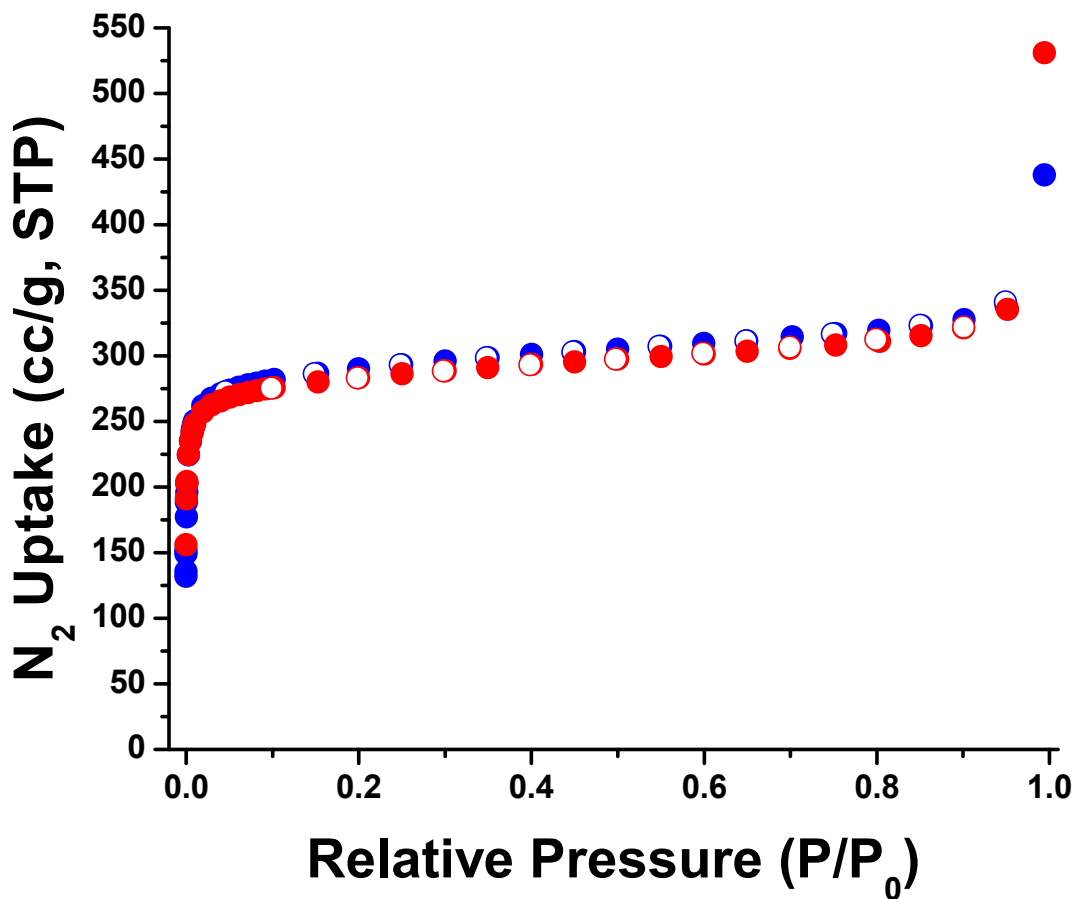


**Figure S19:** N<sub>2</sub> Isotherms (77 K) of **I** activated at 150°C (blue) and 200°C (red).

## 5. MMM Characterization and Performance

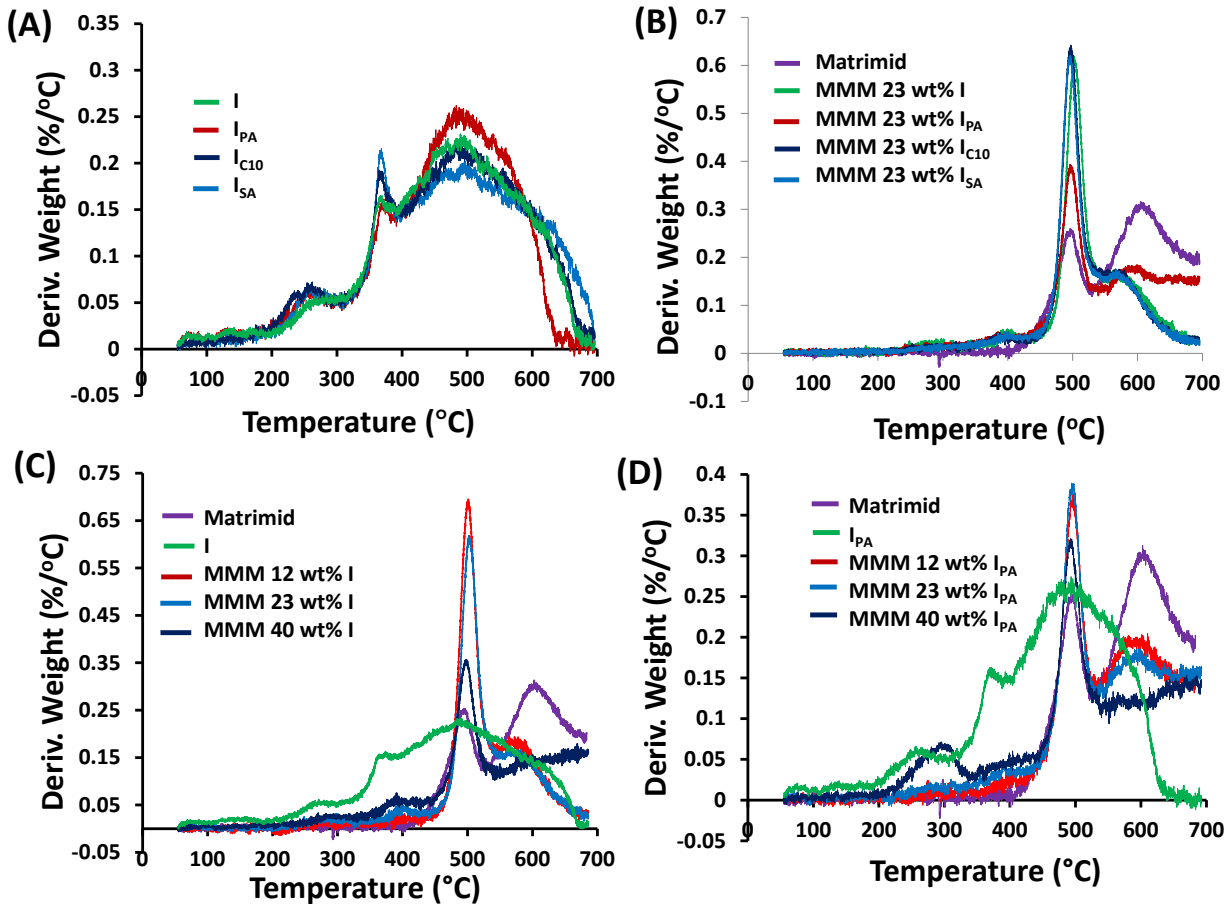


**Figure S20:** Corresponding derivative weight loss to Figure 3 in the manuscript of MOF analogues (A), 23 wt% loaded MMMs (B), MMMs containing varying amounts of I (C), and MMMs containing varying amounts of IPA (D).

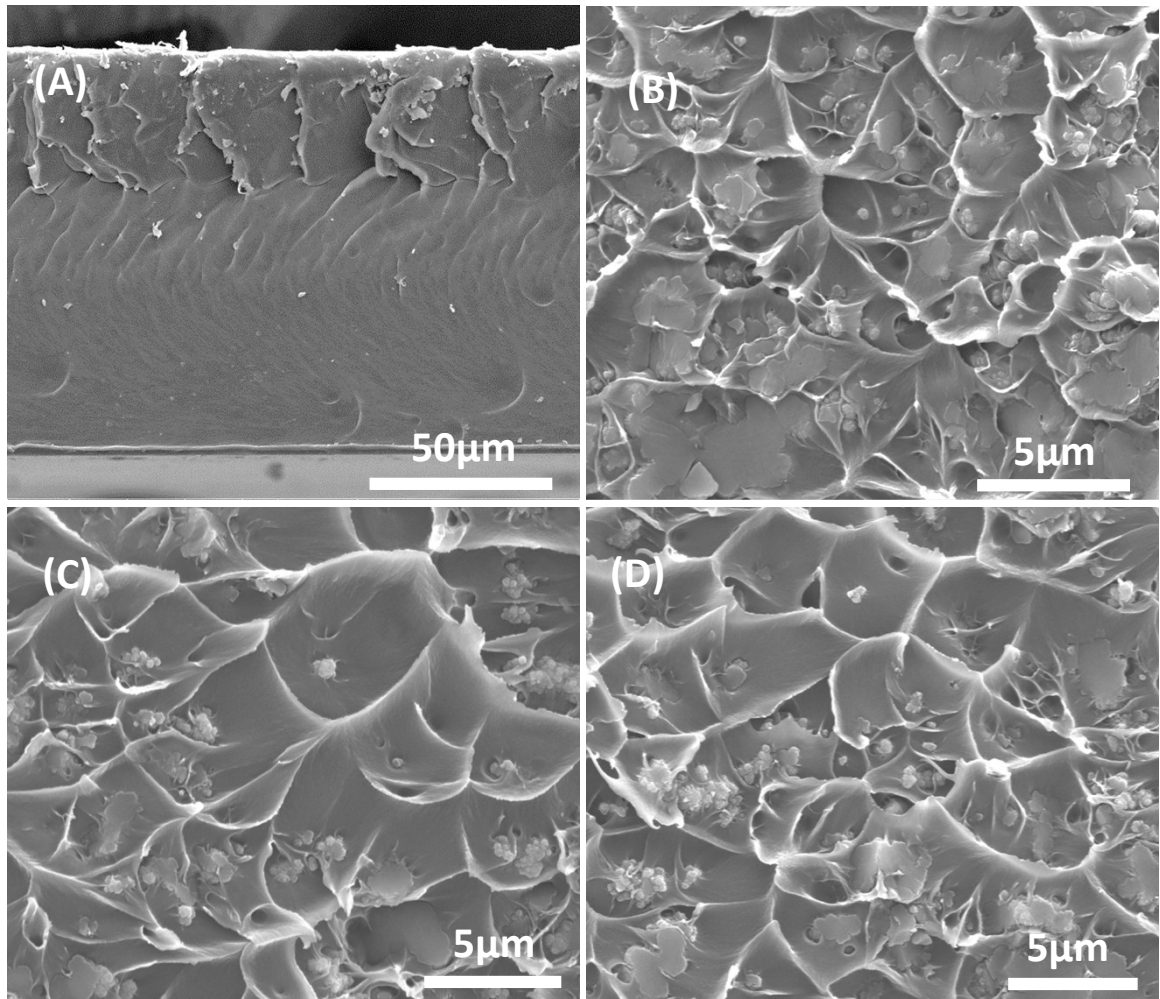


**Figure S21.** SEM images for neat Matrimid<sup>®</sup> (A) and 23 wt% loading of I (B), I<sub>C10</sub> (C), and I<sub>SA</sub> (D) in Matrimid<sup>®</sup>.

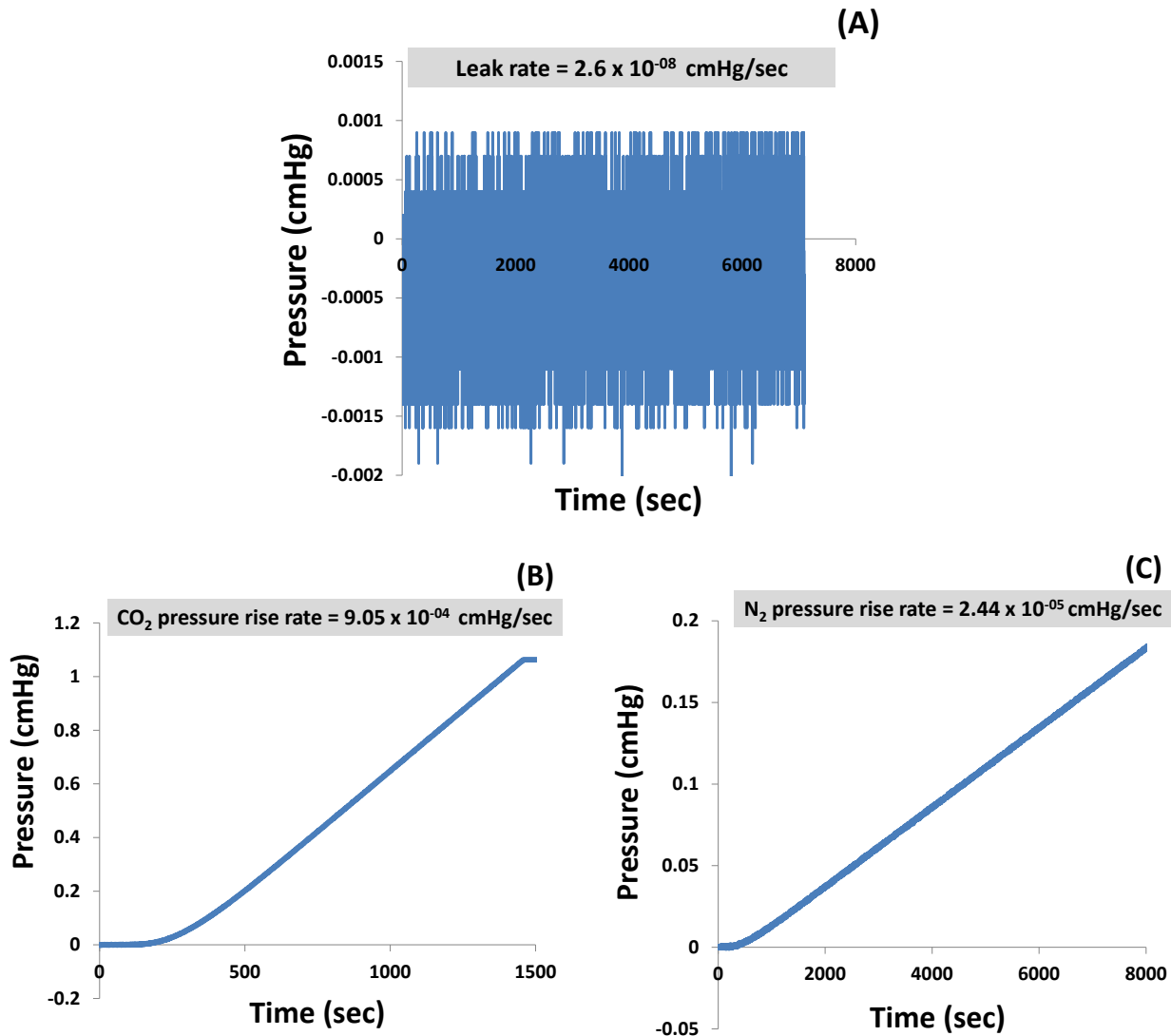


**Figure S22.** Typical pressure rise rates of the isochoric system used in this study: (A) downstream volume leak rate ( $2.6 \times 10^{-8}$  cmHg/sec), (B)  $\text{CO}_2$  steady state pressure rise rate ( $9.1 \times 10^{-4}$  cmHg/sec), and (C)  $\text{N}_2$  steady state pressure rise rate ( $2.4 \times 10^{-5}$  cmHg/sec). Leak rate is at least 3 orders of magnitude less than the test gas ( $\text{CO}_2$  and  $\text{N}_2$ ) pressure rise rates.

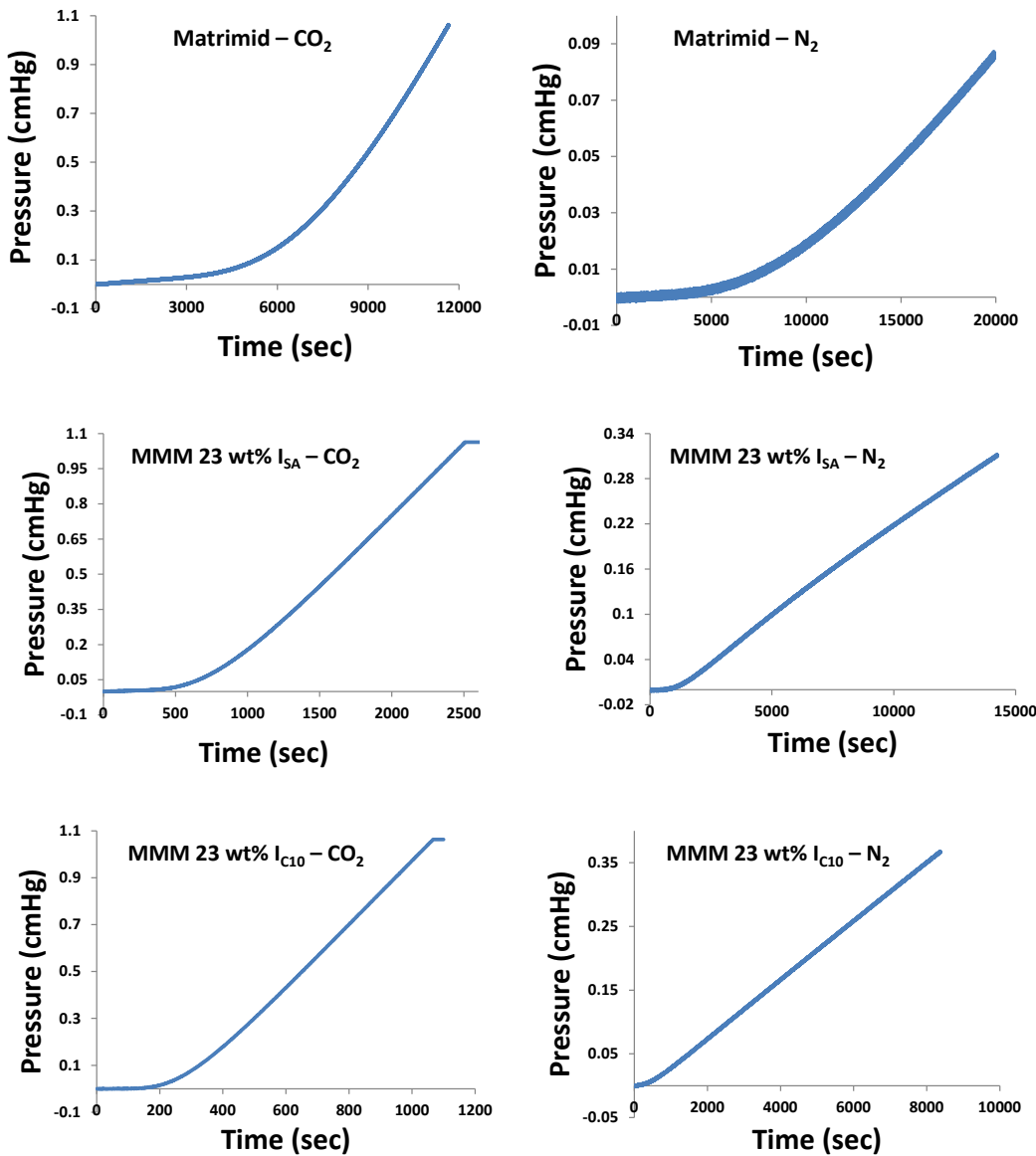


**Figure S23.** CO<sub>2</sub> and N<sub>2</sub> gas downstream pressure rise rates of pure Matrimid, MMM 23 wt% I<sub>C10</sub> and MMM 23 wt% I<sub>SA</sub> membranes tested in the isochoric system. All pressures are absolute pressures.

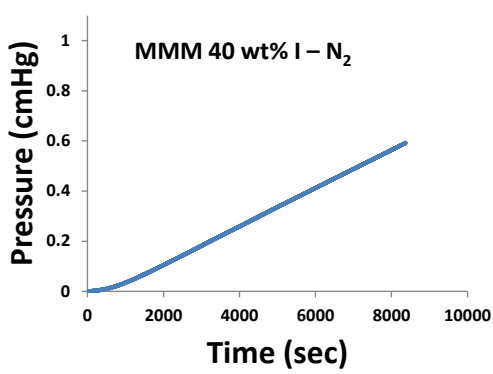
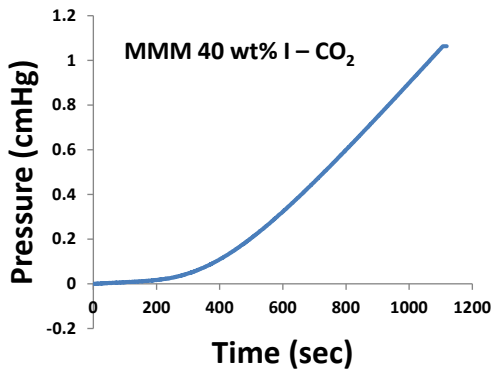
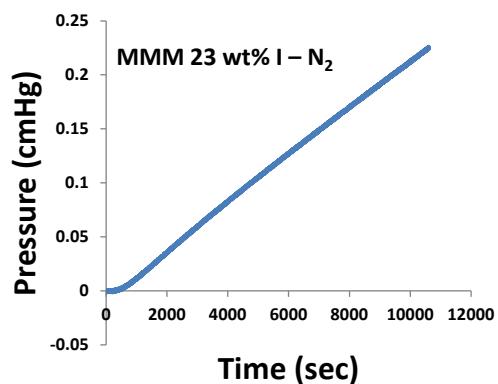
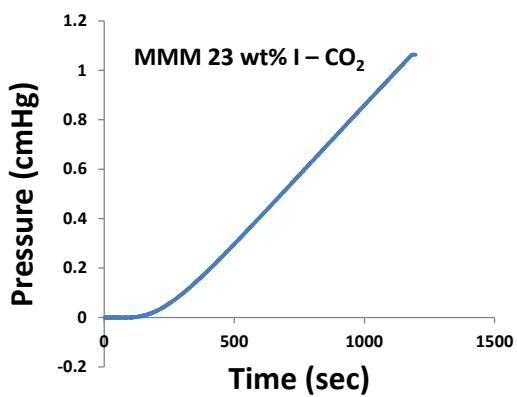
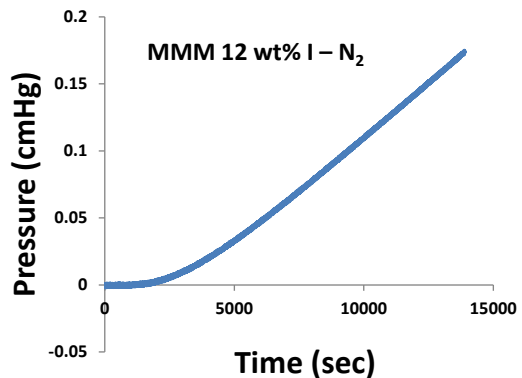
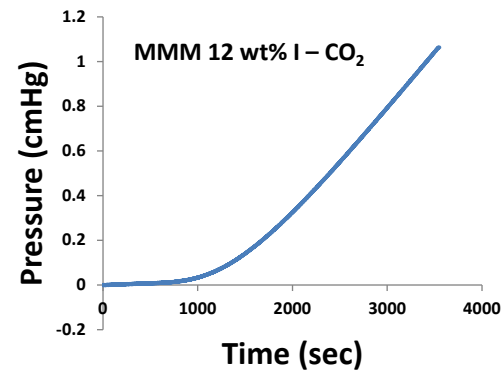


**Figure S24.** CO<sub>2</sub> and N<sub>2</sub> gas downstream pressure rise rates of MMM 12 wt% I, MMM 23 wt% I and MMM 40 wt% I membranes tested in the isochoric system. All pressures are absolute pressures.

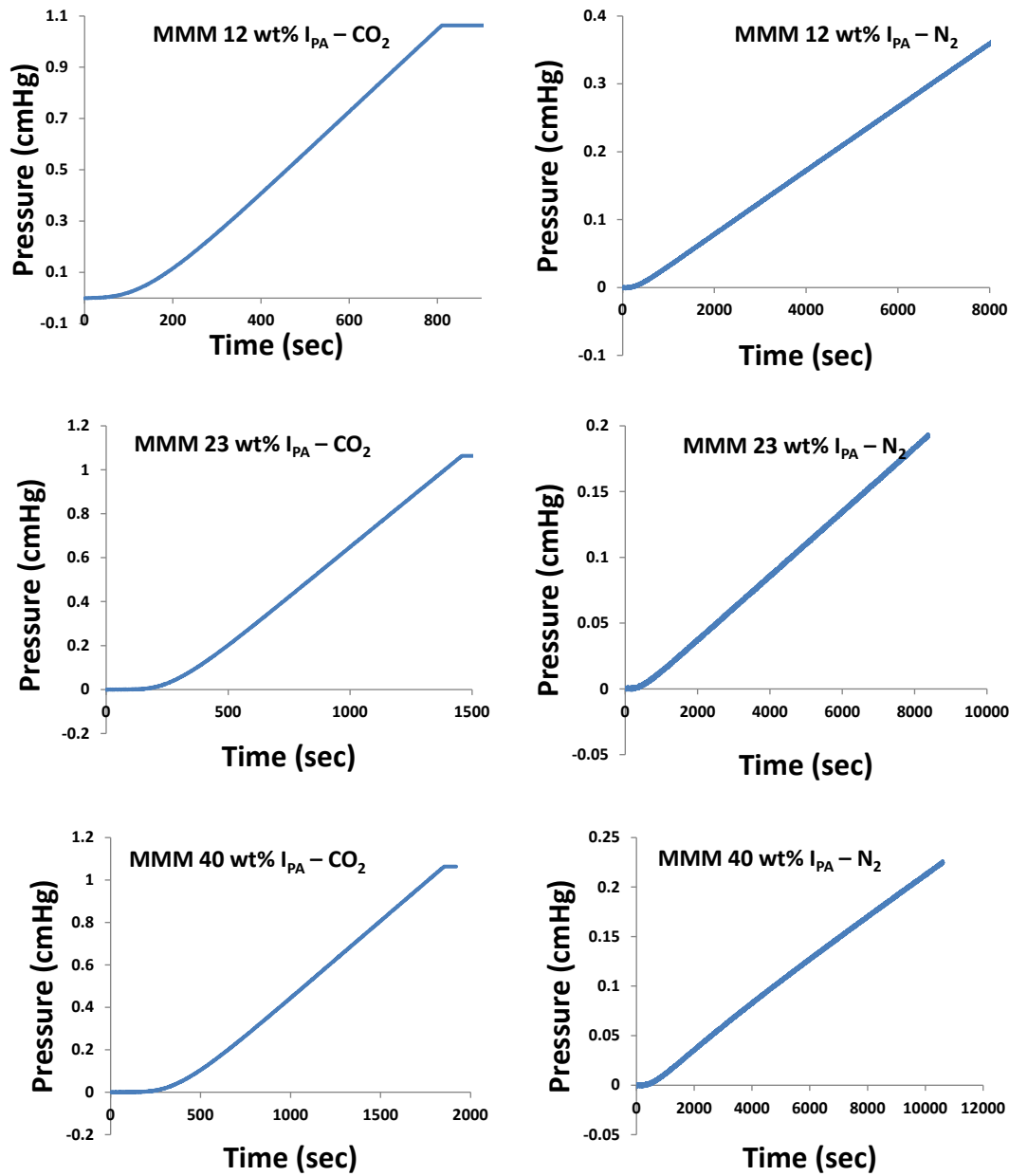


**Figure S25.**  $\text{CO}_2$  and  $\text{N}_2$  gas downstream pressure rise rates of MMM 12 wt%  $I_{PA}$ , MMM 23 wt%  $I_{PA}$  and MMM 40 wt%  $I_{PA}$  membranes tested in the isochoric system. All pressures are absolute pressures.

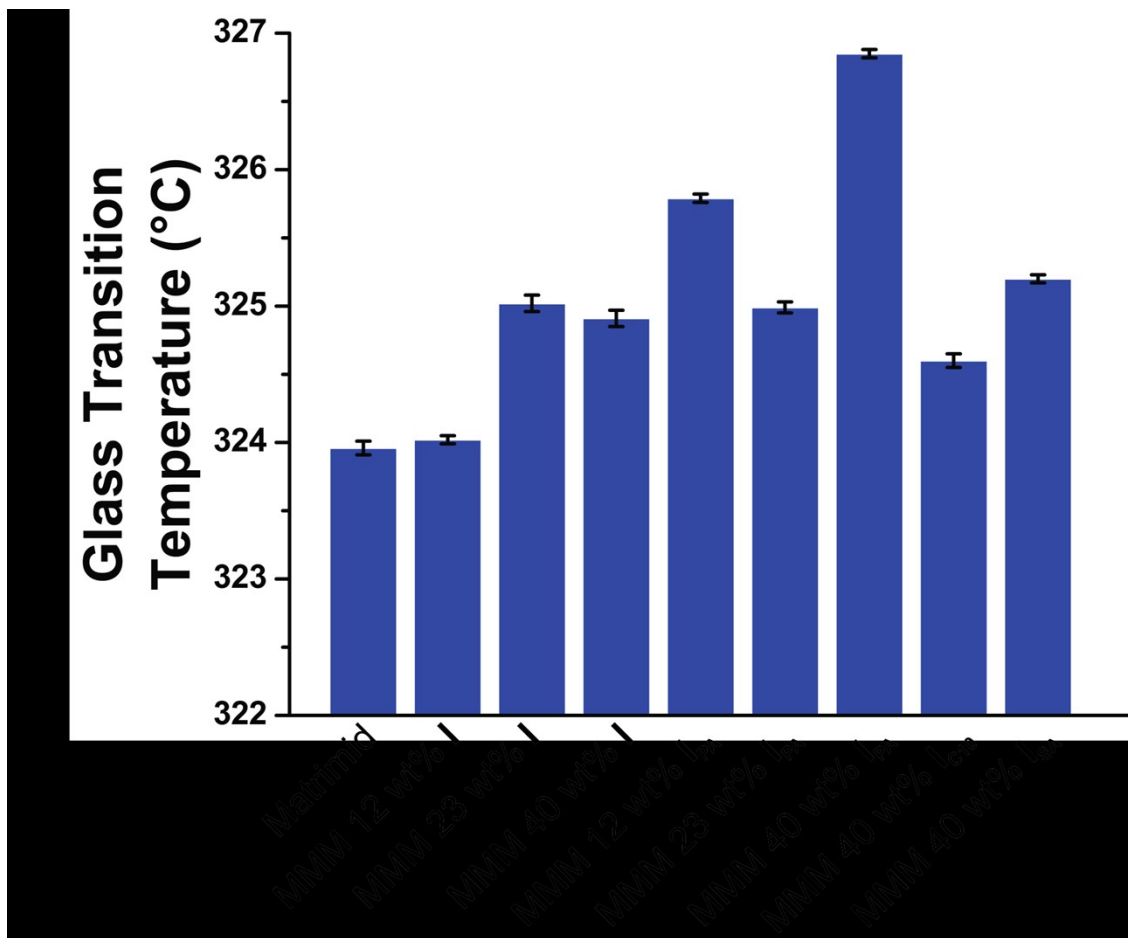


**Figure S26.** Glass transition temperature for membranes containing varying amounts of **I**, **I<sub>PA</sub>**, **I<sub>C10</sub>** and **I<sub>SA</sub>** as determined by DSC.

## 6. Raw Sorption Data Tables

NH <sub>2</sub> -UiO66, I							
CO <sub>2</sub> at 273K		CO <sub>2</sub> at 298K		N <sub>2</sub> at 273K		N <sub>2</sub> at 298K	
P (bar)	Q (cc/g)	P (bar)	Q (cc/g)	P (bar)	Q (cc/g)	P (bar)	Q (cc/g)
0.000340268	0.114168844	0.00109608	0.105233496	0.00107377	0.011683936	0.0010849	0.004564156
0.000389477	0.131093719	0.00305419	0.288220049	0.00534507	0.008395183	0.00743109	0.00886802
0.000503281	0.169978392	0.00511415	0.513193154	0.00743259	0.032310758	0.00951742	0.022089364
0.000741414	0.250429146	0.00708305	0.800391198	0.00951261	0.055286797	0.0105361	0.023307433
0.00105604	0.337824121	0.00917326	1.041330073	0.0105356	0.062570171	0.0299162	0.123293643
0.00107128	0.328826633	0.0103133	1.177645477	0.0298469	0.244355012	0.0528517	0.23797824
0.00311378	0.993726131	0.0144847	1.67403423	0.052798	0.446200489	0.072869	0.334870416
0.0050985	1.613603015	0.0193768	2.241841076	0.0727957	0.617809291	0.0928778	0.431249389
0.00720678	2.252188442	0.0243767	2.804498778	0.09282	0.791212714	0.102927	0.478757946
0.0092382	2.849170854	0.0293951	3.363398533	0.102912	0.879440098	0.152625	0.717694377
0.0101414	3.108140704	0.0415049	4.634914425	0.152422	1.308132029	0.202702	0.928330073
0.0296664	8.069698492	0.0517884	5.679731051	0.202487	1.708855746	0.252631	1.185256724
0.0515868	12.90494975	0.0618496	6.665843521	0.252405	2.151141809	0.302645	1.420929095
0.0718844	16.85502513	0.0718644	7.625672372	0.302475	2.567775061	0.352613	1.679310513
0.0921005	20.42012563	0.0773934	8.154523227	0.35241	3.005354523	0.402637	1.918723716
0.100916	21.90125628	0.0824238	8.633422983	0.402458	3.41806846	0.452634	2.168877751
0.150688	29.1459799	0.0919861	9.491149144	0.452403	3.852836186	0.502632	2.414523227
0.20101	35.27738693	0.101974	10.36354523	0.502436	4.262322738	0.552632	2.654645477
0.251199	40.62638191	0.15234	14.38755501	0.552416	4.672762836	0.602599	2.908410758
0.301373	45.32060302	0.202475	17.9800978	0.602411	5.093667482	0.65261	3.156968215
0.351484	49.55376884	0.252466	21.3398533	0.652389	5.510391198	0.702616	3.395158924
0.401731	53.39623116	0.29939	24.18992665	0.70242	5.921149144	0.752637	3.639364303
0.451949	56.92864322	0.352486	27.2792176	0.75247	6.306968215	0.80264	3.875305623
0.502121	60.1798995	0.399673	29.84498778	0.80241	6.710709046	0.852645	4.112713936
0.552188	63.20351759	0.449707	32.37603912	0.852433	7.102982885	0.902655	4.337897311
0.602236	66.04396985	0.499816	34.799022	0.902451	7.485550122	0.952681	4.563202934
0.65226	68.72085427	0.54996	37.09413203	0.952446	7.866356968	0.997706	4.75801956
0.702299	71.24271357	0.600066	39.30391198	0.997476	8.192933985		
0.752303	73.64221106	0.650151	41.43325183				
0.802296	75.92035176	0.700313	43.43056235				
0.852359	78.09899497	0.750295	45.39144254				
0.899624	80.05326633	0.800449	47.23374083				
0.949558	82.0218593	0.850503	49.04914425				
0.994943	83.76331658	0.900616	50.77090465				
		0.950615	52.4601467				
		0.995966	53.89657702				

**PA-NH<sub>2</sub>-UiO66, I<sub>PA</sub>**

CO <sub>2</sub> at 273K		CO <sub>2</sub> at 298K		N <sub>2</sub> at 273K		N <sub>2</sub> at 298K	
P (bar)	Q (cc/g)	P (bar)	Q (cc/g)	P (bar)	Q (cc/g)	P (bar)	Q (cc/g)
0.00011194	0.029757263	0.000126163	0.012094921	0.00107177	0.011169079	0.00108354	0.005306539
0.000300326	0.086509895	0.000322939	0.03494	0.0107754	0.059258427	0.00744078	0.007244539
0.000540391	0.158590947	0.000521303	0.057668989	0.0298161	0.228651685	0.00953907	0.020104607
0.000729486	0.215981053	0.000720535	0.081653933	0.052704	0.432961798	0.0105585	0.020749865
0.00102164	0.282583158	0.00108234	0.10906427	0.0727726	0.607047191	0.0299258	0.116922247
0.00106584	0.279869474	0.00112566	0.098626067	0.0927507	0.77694382	0.0528702	0.224037978
0.0031078	0.871486316	0.00310363	0.329469663	0.10286	0.867483146	0.0728721	0.317957303
0.00507536	1.421343158	0.0052109	0.569660674	0.152331	1.294588764	0.092882	0.410017978
0.0071756	1.991981053	0.00709646	0.780752809	0.202436	1.691826966	0.102934	0.456694382
0.0092201	2.532484211	0.00914004	1.00985618	0.252317	2.128822472	0.152633	0.684195506
0.0101162	2.761663158	0.0102857	1.135779775	0.302405	2.534157303	0.202701	0.89152809
0.0295779	7.332442105	0.0296013	3.151033708	0.352305	2.966337079	0.252607	1.142746067
0.0513459	11.83195789	0.049922	5.195775281	0.402368	3.380179775	0.302652	1.370152809
0.0716234	15.55877895	0.0701221	7.098539326	0.452344	3.8	0.352621	1.615638202
0.0918107	18.92191579	0.090276	8.888988764	0.502369	4.21047191	0.402649	1.850651685
0.100673	20.32713684	0.101535	9.867640449	0.552355	4.62588764	0.452623	2.096368539
0.15031	27.21936842	0.152051	13.86658427	0.602357	5.039123596	0.502631	2.338719101
0.200688	33.112	0.202093	17.43573034	0.652341	5.455280899	0.552644	2.577775281
0.250914	38.26631579	0.252132	20.75447191	0.702371	5.849730337	0.602623	2.824022472
0.301146	42.82210526	0.302307	23.82382022	0.752407	6.246494382	0.652654	3.067168539
0.351297	46.93726316	0.352438	26.70067416	0.802382	6.635932584	0.702657	3.299483146
0.401457	50.66589474	0.402417	29.39707865	0.852402	7.026404494	0.752599	3.554269663
0.451539	54.11389474	0.45244	31.95707865	0.902388	7.410134831	0.802644	3.787303371
0.501791	57.29221053	0.502457	34.36269663	0.952403	7.781505618	0.852617	4.040988764
0.551951	60.27073684	0.552469	36.6611236	0.997475	8.115865169	0.902672	4.272516854
0.6021	63.07515789	0.59942	38.70966292			0.952659	4.499280899
0.652216	65.69831579	0.652514	40.92292135			0.997585	4.744629213
0.70224	68.16715789	0.699639	42.81460674				
0.752291	70.52926316	0.749596	44.7305618				
0.802302	72.76126316	0.7997	46.57146067				
0.852368	74.88273684	0.84978	48.35797753				
0.902411	76.91305263	0.899905	50.08				
0.952355	78.87178947	0.949999	51.74224719				
0.994776	80.45431579	0.995309	53.20269663				

C <sub>10</sub> -NH <sub>2</sub> -UiO-66, I <sub>C10</sub>							
CO <sub>2</sub> at 273K		CO <sub>2</sub> at 298K		N <sub>2</sub> at 273K		N <sub>2</sub> at 298K	
P (bar)	Q (cc/g)	P (bar)	Q (cc/g)	P (bar)	Q (cc/g)	P (bar)	Q (cc/g)
0.000111678	0.030757023	0.000183853	0.020355191	0.00978408	0.041395349	0.00529504	0.013321685
0.000341583	0.102562683	0.000322986	0.036698517	0.0105009	0.042523256	0.00742239	0.024969803
0.000541566	0.164404612	0.00052171	0.059470763	0.0159196	0.096688372	0.00951231	0.036915098
0.000733565	0.224446541	0.000704192	0.081663347	0.020018	0.134110233	0.010524	0.039713129
0.00101885	0.294184486	0.0011051	0.117472669	0.0249992	0.179558605	0.0299434	0.141380306
0.00106248	0.291513627	0.00111886	0.108880508	0.0299882	0.214547442	0.0528724	0.263472648
0.00308854	0.898073375	0.00309898	0.337341102	0.0428444	0.332576744	0.0728676	0.368070022
0.00504455	1.46442348	0.00521941	0.578923729	0.0528749	0.422237209	0.0928677	0.467124726
0.0071475	2.058333333	0.00710797	0.790595339	0.0628779	0.505693023	0.102939	0.521249453
0.00918808	2.621907757	0.00912849	1.016851695	0.0728887	0.591413953	0.152612	0.774166302
0.0100868	2.86197065	0.0102892	1.145557203	0.0779301	0.636534884	0.202627	1.007770241
0.0294831	7.60408805	0.0295287	3.143432203	0.0829355	0.677230233	0.252563	1.280516411
0.0510887	12.29756813	0.0497288	5.159004237	0.0928931	0.75962093	0.30261	1.532538293
0.0713608	16.23113208	0.0699156	7.048983051	0.102865	0.844513953	0.352578	1.802183807
0.0914745	19.77981132	0.0900328	8.835487288	0.152359	1.275225581	0.402589	2.054796499
0.100431	21.27924528	0.101397	9.815233051	0.202427	1.679923256	0.452558	2.331247265
0.149696	28.56582809	0.151848	13.81154661	0.252354	2.121283721	0.502583	2.596695842
0.200085	34.87316562	0.201937	17.38911017	0.302396	2.536651163	0.552564	2.858358862
0.250376	40.40356394	0.251951	20.71565678	0.352349	2.971023256	0.602542	3.132647702
0.300667	45.27987421	0.301987	23.78495763	0.402355	3.396651163	0.65255	3.396870897
0.350843	49.68888889	0.352194	26.69025424	0.452343	3.824465116	0.702538	3.667592998
0.401053	53.6884696	0.402292	29.40360169	0.502389	4.235325581	0.752552	3.93428884
0.451185	57.37379455	0.452329	31.97775424	0.552351	4.654930233	0.802571	4.185886214
0.501303	60.77589099	0.502354	34.39851695	0.602382	5.071162791	0.852562	4.454245077
0.551525	63.95702306	0.552367	36.71122881	0.65239	5.475046512	0.902571	4.704682713
0.601771	66.94150943	0.602437	38.91016949	0.702389	5.872883721	0.952544	4.961400438
0.651954	69.74800839	0.652416	41.02605932	0.752391	6.278534884	0.997615	5.177964989
0.702028	72.40712788	0.702439	43.03665254	0.802397	6.672023256		
0.752146	74.90293501	0.752437	44.98389831	0.852416	7.059581395		
0.802173	77.27840671	0.799555	46.73411017	0.902402	7.439604651		
0.852185	79.55786164	0.852458	48.63813559	0.952482	7.788162791		
0.902217	81.73186583	0.8997	50.27521186	0.997441	8.130139535		
0.952271	83.79098532	0.949671	51.92860169				
0.997295	85.59392034	0.995024	53.39194915				

SA-NH <sub>2</sub> -UiO-66, I <sub>SA</sub>							
CO <sub>2</sub> at 273K		CO <sub>2</sub> at 298K		N <sub>2</sub> at 273K		N <sub>2</sub> at 298K	
P (bar)	Q (cc/g)	P (bar)	Q (cc/g)	P (bar)	Q (cc/g)	P (bar)	Q (cc/g)
0.000121067	0.032313433	0.000446868	0.038958191	0.0010808	0.006777616	0.00108303	0.004636364
0.000301358	0.08585995	0.000456752	0.034974572	0.00740924	0.018280754	0.0074452	0.005036364
0.000538368	0.163125622	0.000524991	0.034133007	0.00950405	0.035057664	0.00950244	0.021218182
0.000737542	0.228746517	0.00070902	0.046177262	0.0105164	0.038834307	0.0105642	0.017072727
0.00105301	0.326124378	0.00115022	0.036234963	0.0299168	0.148311192	0.0299148	0.104290909
0.00107276	0.336012438	0.00302571	0.150047922	0.0528564	0.279985401	0.052835	0.210218182
0.00305758	0.979726368	0.00507012	0.336711491	0.0728972	0.390530414	0.0728341	0.299309091
0.00502653	1.599554726	0.00717599	0.525462103	0.0928738	0.499754258	0.0928461	0.386381818
0.0071619	2.226927861	0.00922587	0.710327628	0.102933	0.556693431	0.102911	0.434272727
0.00922345	2.804577114	0.0103405	0.801757946	0.152599	0.829525547	0.152528	0.666181818
0.0101424	3.061293532	0.0297185	2.514743276	0.202664	1.079919708	0.202617	0.876545455
0.0297101	7.090671642	0.0505736	4.265721271	0.252623	1.355340633	0.252499	1.125981818
0.0518712	11.0258209	0.0708006	5.848459658	0.302664	1.609097324	0.302575	1.350309091
0.0721143	14.21524876	0.0909411	7.326234719	0.352601	1.888111922	0.35251	1.599054545
0.089446	16.68753731	0.101886	8.135281174	0.402652	2.152776156	0.402513	1.8386
0.100751	18.25430348	0.152399	11.36704156	0.452613	2.429218978	0.452467	2.091454545
0.150963	24.08838308	0.202449	14.24645477	0.502637	2.703017032	0.502509	2.334090909
0.201179	29.0420398	0.249241	16.76154034	0.55261	2.975206813	0.552464	2.588127273
0.25131	33.43258706	0.299253	19.23596577	0.602664	3.239781022	0.602494	2.835436364
0.30155	37.34079602	0.349421	21.59317848	0.65258	3.529562044	0.65241	3.095909091
0.35173	40.91467662	0.399601	23.80254279	0.702659	3.785498783	0.702491	3.337054545
0.401951	44.19402985	0.449701	25.92298289	0.752642	4.040681265	0.752447	3.588927273
0.451998	47.23706468	0.499871	27.92787286	0.802669	4.301313869	0.802439	3.836563636
0.502055	50.05970149	0.549937	29.8608802	0.852653	4.551654501	0.852477	4.080054545
0.552106	52.70621891	0.600073	31.71075795	0.90268	4.79406326	0.902486	4.320072727
0.602155	55.20771144	0.650154	33.5002445	0.952664	5.034987835	0.952431	4.569381818
0.649242	57.42910448	0.700262	35.199022	0.997686	5.254306569	0.997509	4.783272727
0.699203	59.67462687	0.750308	36.86332518				
0.749329	61.81766169	0.800388	38.46479218				
0.799469	63.86567164	0.850426	40.03080685				
0.849569	65.83208955	0.900537	41.5396088				
0.899648	67.72960199	0.950556	43.0200489				
0.949808	69.53781095	0.995837	44.32762836				
0.995165	71.13532338						

1. A. L. Myers and J. M. Prausnitz, *AIChE Journal*, 1965, **11**, 121-127.